Technical University of Denmark

DTU

Stylolites, porosity, depositional texture, and silicates in chalk facies sediments
Ontong Java Plateau - Gorm and Tyra fields, North Sea

Fabricius, Ida Lykke; Borre, Mai K.

Link back to DTU Orbit

DTU Library
Technical Information Center of Denmark

Stylolites, porosity, depositional texture, and silicates in chalk facies sediments. Ontong Java Plateau – Gorm and Tyra fields, North Sea

IDA L. FABRICIUS and MAI K. BORRE[1]
Institute of Environment and Resources, Technical University of Denmark, Bygningstorvet 115, DK-2800 Kgs. Lyngby, Denmark (E-mail: ilf@er.dtu.dk)

ABSTRACT

Comparison of chalk on the Ontong Java Plateau and chalk in the Central North Sea indicates that, whereas pressure dissolution is controlled by effective burial stress, pore-filling cementation is controlled by temperature. Effective burial stress is caused by the weight of all overlying water and sediments as counteracted by the pressure in the pore fluid, so the regional overpressure in the Central North Sea is one reason why the two localities have different relationships between temperature and effective burial stress. In the chalk of the Ontong Java Plateau the onset of calcite-silicate pressure dissolution around 490 m below sea floor (bsf) corresponds to an interval of waning porosity-decline, and even the occurrence of proper stylolites from 830 m bsf is accompanied by only minor porosity reduction. Because opal is present, the pore-water is relatively rich in Si which through the formation of Ca–silica complexes causes an apparent super-saturation of Ca and retards cementation. The onset of massive pore-filling cementation at 1100 m bsf may be controlled by the temperature-dependent transition from opal-CT to quartz. In the stylolite-bearing chalk of two wells in the Gorm and Tyra fields, the nannofossil matrix shows recrystallization but only minor pore-filling cement, whereas microfossils are cemented. Cementation in Gorm and Tyra is thus partial and has apparently not been retarded by opal-controlled pore-water. A possible explanation is that, due to the relatively high temperature, silica has equilibrated to quartz before the onset of pressure dissolution and thus, in this case, dissolution and precipitation of calcite have no lag. This temperature versus effective burial stress induced difference in diagenetic history is of particular relevance when exploring for hydrocarbons in normally pressured chalk, while most experience has been accumulated in the over-pressured chalk of the central North Sea.

Keywords Cementation, chalk, diagenesis, North Sea, Ontong Java Plateau, porosity, stylolites.

INTRODUCTION

Cementation of chalk during burial diagenesis requires a source of carbonate and it is generally accepted that pressure dissolution plays a major role (e.g. Scholle, 1977; Bathurst, 1995), but it remains an issue of debate how temperature and pressure controls this process, and whether clay minerals promote the process (e.g. Heald, 1955; Simpson, 1985; Lind, 1993a; Sheldon *et al.*, 2003; Safaricz & Davison, 2005). It also remains unclear how diagenetically controlled changes in the mineralogy of silicates in the chalk influence

[1]Present address: Mærsk Olie og Gas A/S, Copenhagen, Denmark.

changes in the dominating carbonate phase (Baker *et al.*, 1980; Hobert & Wetzel, 1989). Finally presence of hydrocarbons may have an influence on the diagenetic process (Scholle, 1977).

Diagenetic processes are controlled by temperature, burial stress and pore-pressure, so, by comparing two settings where some but not all of these conditions differ, the understanding of chalk diagenesis and porosity development during burial should be improved. The two settings are the chalk facies sediments and sedimentary rocks of the Ontong Java Plateau as found in Ocean Drilling Program (ODP) Leg 130 Site 807 (no hydrocarbons) and chalk of the Central North Sea as found in two wells of the Gorm and Tyra fields (hydrocarbon bearing).

The main components of pelagic chalk are calcareous nannofossils and microfossils. Due to the contrast in size between these fossils, microfossils reside in a continuous matrix of nannofossils. In the North Sea area, chalk facies sediments of the Upper Cretaceous and Palaeogene Chalk Group are commonly referred to as 'chalk' irrespective of degree of induration. This may cause confusion when comparison is made to pelagic deep sea carbonate sediments. These sediments and sedimentary rocks of Cretaceous to Present age are of chalk facies and very similar in appearance and composition to North Sea chalk, but they are described as carbonate ooze, chalk or limestone as a reflection of increasing induration (Mazzullo *et al.*, 1988). In the discussion of diagenesis a distinction is made between recrystallization and pore-filling cementation. Recrystallization involves local simultaneous dissolution of carbonate particles and overgrowth on carbonate particles, where no net transport of Ca^{2+} and CO_3^{2-} is required and no porosity change necessarily is involved, whereas pore-filling cementation is a result of diffusion and net precipitation of material derived, e.g. from dissolution at stylolites (Borre & Fabricius, 1998).

The present paper includes a discussion of the role of temperature and stress on stylolite formation, and the role of clay minerals in pressure dissolution. It also discusses the mainly porosity-neutral process of recrystallization, as well as pore-filling cementation, and how these processes are related to depositional texture and the non-carbonate components of the chalk. Finally the effect of these processes on porosity and permeability is discussed.

SAMPLES AND METHODS

Ontong Java Plateau

Ooze and chalk with colour bands as well as chalk and limestone with stylolites were sampled from Site 807 during ODP Leg 130 (Fig. 1). Part of each sample was impregnated with epoxy resin and polished before backscatter electron micrography using a Philips XL40 scanning electron microscope (Philips, Holland). Silica and barite were analysed by wavelength dispersive microprobe analysis using a JEOL Superprobe 733 (JEOL, Japan). Standards were: quartz, barite, celestite, and calcite.

Another part of each sample was soaked in demineralized water and slowly leached by acetic acid, while controlling the pH to be above 5·5 in order to prevent dissolution of all non-carbonates. The filtrate was analysed for Al, Fe, Mg, Si, and Sr by Atom Absorption Spectroscopy (Perkin-Elmer 5000, CT, USA). The residue was analysed for mineralogical composition by X-ray diffraction by use of Cu K-α radiation over an interval of 2Θ 2° to 60°. Diffractograms were also recorded from 2° to 30° subsequent to 3 days of glycolation at 60 °C, and subsequent to heating to 300 °C and to 500 °C respectively in order to identify clay minerals.

Image analysis was done on backscatter electron micrographs of impregnated polished samples also studied by Borre & Fabricius (1998), to measure nannofossil matrix porosity, and amounts of large particles (e.g. foraminifers) and pores by use of the filtering method described by Borre (1997; Figs 2 and 3). Samples, visually free of stylolites or colour bands, were analysed for specific surface area using N_2 adsorption (BET) with a MicromeriticsGemini III 2375 surface area analyser (GA, USA).

Gorm and Tyra fields

Plug samples from Gorm Field well N-22X and Tyra Field well E-5X (Fig. 1) were chosen, so that for most samples He-porosity data were available from the operator. Ultrasonic velocity data of the samples were discussed by Borre (1998). The majority of the Gorm Field samples were discussed with respect to specific surface and permeability by Mortensen *et al.* (1998). The Tyra samples were discussed with respect to image analysis by Røgen *et al.* (2001), and with respect to permeability and capillary entry pressure by Røgen & Fabricius (2002). In the present study backscatter electron micrographs from all se-
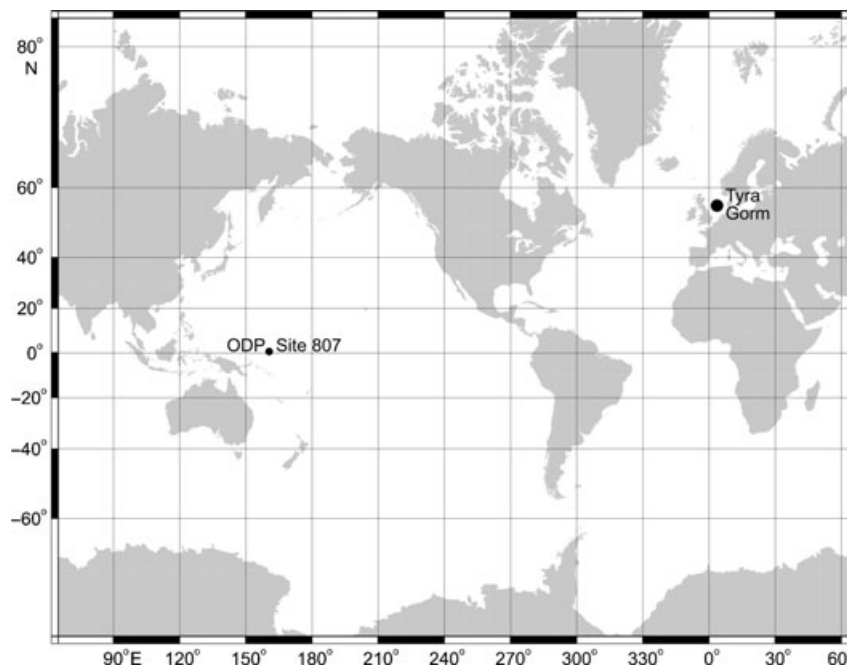
Fig. 1. Location of studied wells: The Ontong Java Plateau, Ocean Drilling Program Leg 130, Site 807, Gorm Field well N-22X, and Tyra Field well E-5X (modified after http://www-odp.tamu.edu/sitemap/ sitemap.html).

lected samples were analysed to measure matrix porosity and amount of large particles and pores by use of the filtering method described by Borre (1997; Fig. 3); and to measure specific surface by use of the filtering method described by Borre *et al.* (1997).

CASE SETTINGS

Ontong Java Plateau – description of facies and case setting

The Ontong Java Plateau is a large oceanic basaltic plateau situated in the western Pacific Ocean (Fig. 1). The thick cover of pelagic carbonates holds no accumulations of hydrocarbons, but has been penetrated several times by the Deep Sea Drilling Project (DSDP) and the ODP (Winterer *et al.*, 1971; Moberly *et al.*, 1986; Kroenke *et al.*, 1991; Mahoney *et al.*, 2001). ODP Site 807 cored more than 1300 m of pelagic carbonate sediments spanning the entire range from Late Cretaceous to present. The upper 293 m of the sediment is composed of nannofossil ooze, overlying 805 m of nannofossil chalk followed by 253 m of nanno-fossil limestone (Fig. 2; Kroenke *et al.*, 1991). The main component of the sediments is calcareous nannofossils, which constitute the matrix of the mud- and wackestones. The second most import-ant constituent is calcareous microfossils, which may be seen as composed of large particles and large pores (Fig. 3; Bachman, 1984). Below 1135 m below sea floor (bsf) in the limestone interval, several beds of re-deposited sediment were recorded, as indicated by intra-clasts, silicate clasts, and slump structures (Kroenke *et al.*, 1991). The temperature of the OJP ranges from around 0 °C at the sea bottom to around 20 °C at 1 km bsf (estimate based on wireline logging data) and the lower part of the OJP chalk is under an effective vertical stress of 8–10 MPa (Fabricius, 2003).

ODP Site 807 is especially suited for the study of burial diagenesis due to the presumed simple subsidence history and drainage equilibrium of the OJP (Table 1). When interpreting the dia-genetic history from well data in the Ontong Java Plateau, it is assumed that primary variations in nannofossil assemblages and size can be disre-garded. Porosity-decline in the upper 600 m of ooze and chalk is caused by mechanical compac-tion, as confirmed by loading experiments (Fig. 4; Lind, 1993b; Fabricius, 2003). Simultaneously with mechanical compaction, recrytallization of calcite crystals causes particles to become more equant, making way for further mechanical com-paction (Fig. 4; Borre & Fabricius, 1998). Image analysis of backscatter electron micrographs in-dicates that the recrystallization causes the sur-face relative to volume (specific surface) of particles to decline; however, the compaction counteracts this effect on pores and causes spe-cific surface of pores to decline only a little. Below 600 m bsf follows an interval of near
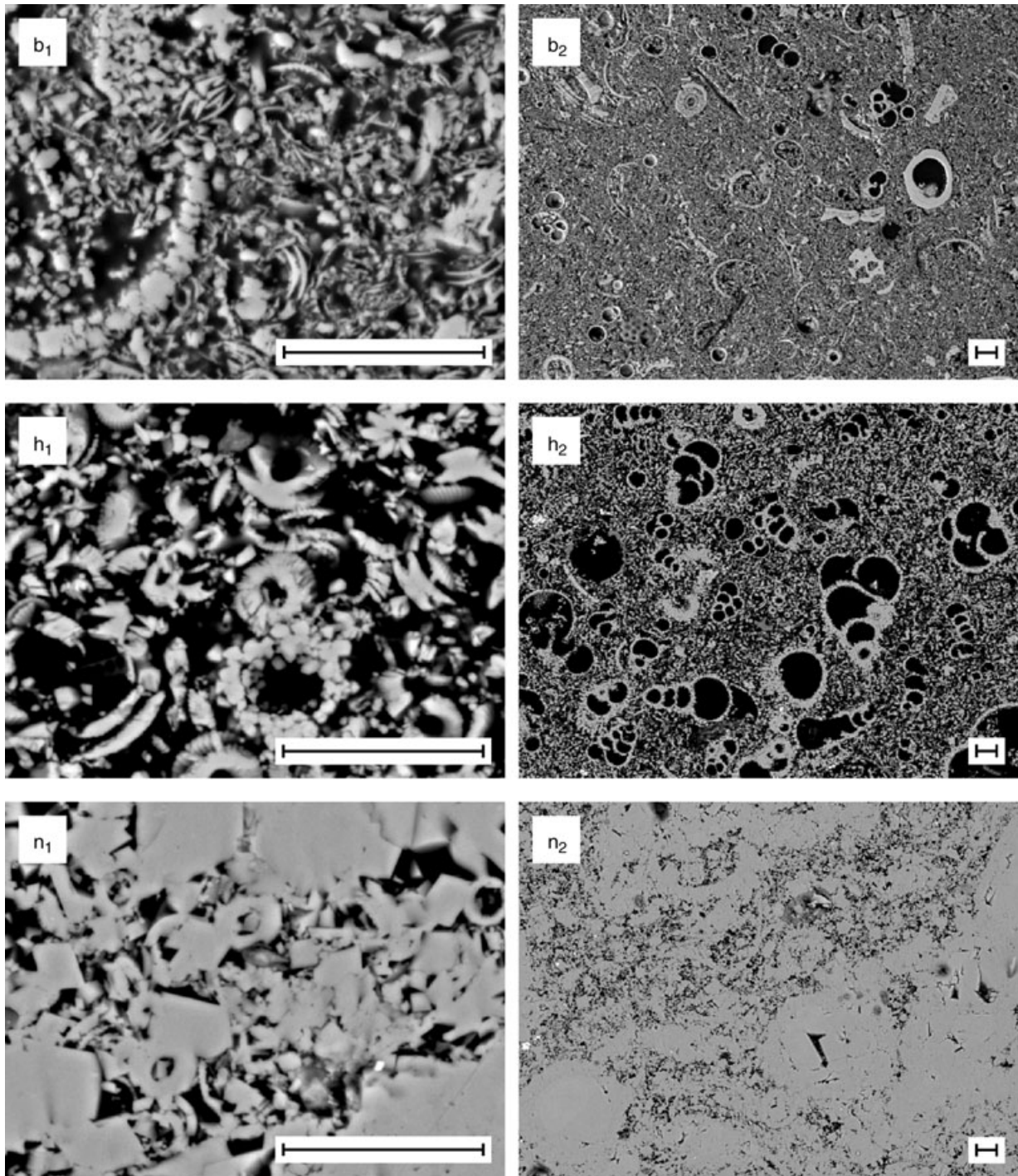
Fig. 2. Ontong Java Plateau, Leg 130, Site 807. Recrystallization and pore-filling cementation. Scale bar is 16 microns. Backscatter electron micrographs: calcite is light grey and pore space is black. (For letters refer to Fig. 4.) (b) 807A-11H-5; Lower Pliocene, depth: 100 m bsf, $CaCO_3$: 93·1%, ϕ_{lab}: 65·5%, ϕ_{matrix}: 66·8%. Ooze, particles are in physical contact and they are partly recrystallized. (h) 807C-6R-1; Lower Oligocene, depth: 829 m bsf, $CaCO_3$: 94·9%, ϕ_{lab}: 55·1%, ϕ_{matrix}: 58·3%. Chalk, particles are connected by internal cement resulting from recrystallization, which has also allowed particles and pore size to increase. (n) 807C-48R-1; Upper Palaeocene, depth: 1146 m bsf, $CaCO_3$: 97·9%, ϕ_{lab}: 14·8%, ϕ_{matrix}: 19·8%. Limestone, microfossils and matrix pore space partly filled by cement, probably externally derived from stylolites.
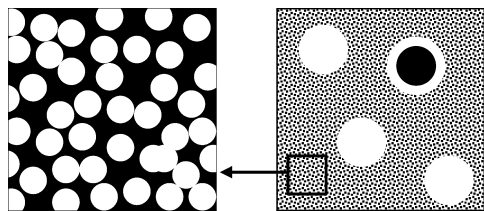
Fig. 3. Conceptual sketch of backscatter electron micrographs of chalk (Røgen, 2002). Left: At high magnification small particles (white) and small pores (black) are seen. They constitute the chalk matrix, and porosity as measured in this image will be the matrix porosity. Right: At low magnification the matrix is blurred, whereas large particles and cemented areas are white, and large porosity is black. Upon repeated filtering, the amount of large particles and cemented areas, as well as large pores can be measured by image analysis (Borre, 1997).

Table 1. Diagenetic processes in chalk facies sediments and sedimentary rocks of Ontong Java Plateau.

Depth (m bsf)	
0–293	Pelagic carbonate ooze lithology
0–600	Mechanical compaction causes porosity decrease
0–490	Sediment contains green and purple colour bands
0 to *ca* 200	Recrystallization dominates specific surface of particles and pores, below this depth decreasing influence along with that of mechanical compaction
ca 200–600	Mechanical compaction dominates specific surface of particles and pores
293–1098	Chalk lithology
490–830	Sediment contains coloured flaser structures
600–950	Porosity roughly constant, while pores and particles grow
780–950	Transition from opal-A to opal-CT
830–	Sediment contains grey flaser structures and stylolites
959–	Sediment contains chert
1098–	Limestone lithology
1127–	Quartz is the only silica phase

constant porosity, where declining specific surface of pores and particles indicates increasing particle- and pore size resulting from recrystallization (Fig. 4; Fabricius, 2003). Around 1100 m bsf, pore-filling cementation by continuous overgrowth causes porosity to decline and specific surface of particles to fall, while specific surface of pores rises (Fig. 4; Borre & Fabricius, 1998).

The carbonate of Ontong Java Plateau is low-Mg calcite. With respect to the non-carbonate com-ponents, the upper 490 m of the ooze and chalk contain up to centimetre-wide green and purple colour bands (Kroenke *et al.*, 1991), the colouring of green bands is due to finely disseminated green silicates probably of volcanic origin, the colouring of purple bands is due to disseminated pyrite (Lind *et al.*, 1993). The distribution of bands may reflect variations in plankton productivity (Berger & Lind, 1997). Below 490 m bsf the colour bands are replaced by more distinct coloured flaser structures, these are again replaced by grey flaser structures and stylolites below 830 m bsf (Figs 5 and 6; Lind, 1993a). The occurrence of stylolites is associated with the onset of pore filling calcite cementation in equilibrium with pore water as reflected in the trend to lower $\delta^{18}O$ values in bulk carbonate samples (Fig. 6; Lind, 1993a). Opaline chert is found from 959 m bsf in the lower part of the chalk section and in the limestone (Fig. 6; Kroenke *et al.*, 1991).

North Sea chalk, Gorm and Tyra fields – description of facies and case setting

Gorm and Tyra fields are structural traps in the chalk of Danish North Sea. Gorm is an oil field with Maastrichtian chalk as the main reservoir (Hurst, 1983), whereas Tyra is primarily a gas field with Danian chalk as the main reservoir (Doyle & Conlin, 1990).

Gorm field well N-22X cored 122 m of chalk of Late Cretaceous (Maastrichtian) and Palaeogene (Danian) age, whereas Tyra field well E-5X cored 24 m of chalk of Palaeogene (Danian) age. The chalk of the North Sea resembles the OJP chalk by containing well-sorted mudstones as well as less well-sorted wackestones. The Gorm and Tyra fields are structures with relatively low relief, so that a heavy influence on diagenesis from advecting waters seen over salt piercement structures is not expected (Jensenius, 1987). Please note that the chalk fields of the North Sea vary with respect to degree of recrystallization and pore-filling cementation, so the two wells in Gorm and Tyra fields are not necessarily typical.

Due to the regional overpressure in the central North Sea (e.g. Japsen, 1998), the effective stress in the North Sea chalk of the Gorm and Tyra fields is comparable with the effective stress at the deeper interval of the OJP (*ca* 10 MPa). They differ though with respect to temperature and age. Mainly due to the deeper burial of the North Sea chalk, the temperature is higher (*ca* 70 °C) than at OJP. Loading experiments on samples from nearby Gorm field well indicate that this chalk
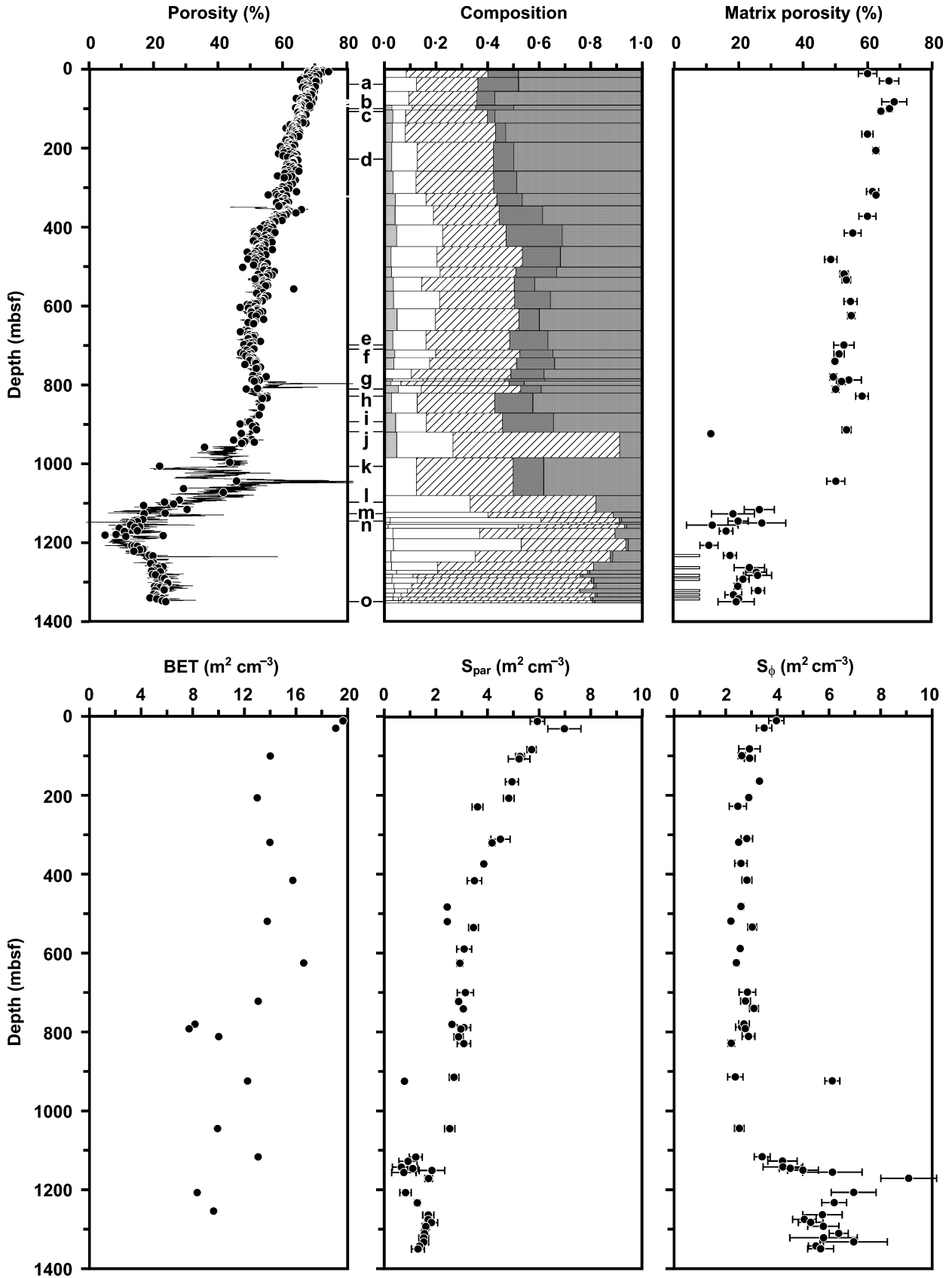
Fig. 4. Data from ODP Site 807. Porosity is from shipboard physical properties data on discrete samples (dots) and calculated from the density log (solid line) (Kroenke *et al.*, 1991). Composition is from analysis of BSE-images. Signatures from left to right indicate; light grey: silicates, white: large particles or large cemented area, hatched: small particles, dark gray: large porosity, medium grey: small porosity (Fig. 2 and 3). Matrix porosity is from image analysis (Figs 2 and 3; Borre & Fabricius, 1998), intraclast-bearing samples are indicated by small bars. BET is specific surface as measured by N_2 adsorption. S_{par} and S_ϕ are specific surface as measured by image analysis with reference to particles, respectively porosity (Borre & Fabricius, 1998).

does not undergo mechanical compaction at its present effective burial (Olsen, 2002).

The chalk of the Gorm and Tyra fields is composed of low-Mg calcite. It contains stylolites resembling those of the OJP with respect to drape thickness and amplitude (Fig. 7). In the Gorm Field stylolite drapes are primarily composed of kaolinite and quartz (Lind *et al.*, 1994), but non-carbonates of the Tyra and Gorm fields include smectite as well as kaolinite and quartz (Røgen & Fabricius, 2002).

RESULTS

Colour bands, flasers and stylolites of Ontong Java Plateau

The green colour bands of the ooze and upper chalk section of the OJP are difficult to recognize on backscatter electron micrographs (Fig. 8). Nevertheless, detailed microprobe analysis allows the identification of dispersed, up to 10 micron-size Fe-bearing, possibly volcanigenic clay particles (Lind *et al.*, 1993). The following minerals were identified in colour band-samples by X-ray diffraction: smectite-chlorite (all samples) which probably gives rise to the green colouring; quartz, albite (most samples) and illite (single samples), which probably are air-blown (Krissek & Janecek, 1993); as well as barite and pyrite (single samples) with crystal shape indicating authigenic origin. All samples contain biogenic opal-A (Figs 6 and 8–10).

With depth, the colour bands become more distinct and wispy until from 490 to 830 m bsf they may be described as green-coloured flaser structures (Fig. 5). Concurrently, the chlorite-peak disappears from the X-ray diffractograms and the clay seems to be only smectite. These flaser structures are discernible in backscatter electron micrographs (Fig. 8). Dissolution of calcitic microfossils at contacts with silicates is visible. The non-carbonate fraction of the sediment is dominated by smectite and biogenic opal-A; and in addition small amounts of probably airborne quartz and albite, as well as authi-

genic barite (Figs 9 and 11). Dolomite was not detected.

From around 830 m bsf the flaser structures are grey. They are now easily visible in backscatter electron micrographs (Fig. 8). Well-developed stylolites with columns and clay drapes are found from 830 m bsf (Fig. 8). The dominating non-carbonates are still smectite and opal, but from around 780 m bsf down to around 950 m bsf, opal-A is gradually replaced by opal-CT.

Silica and silicates

In the entire carbonate section cored in ODP Site 807, quartz is found as a minor, probably wind-borne constituent (Krissek & Janecek, 1993), but biogenic opal-A dominates in the upper section, before being replaced by opal-CT in the depth interval 780–950 m bsf. In this depth interval, the chalk has an Oligocene age corresponding to 31–43 Ma (Kroenke *et al.*, 1991), and an estimated temperature of 15–20 °C. In line with the observations of Hobert & Wetzel (1989), the transition from opal-A to opal-CT is accompanied by a fall in specific surface of the sediment as measured by BET (Fig. 4).

Down to around 950 m bsf the amount of dissolvable Si decreases in the sediment, concurrent with an increase in Si-concentration in the pore water (Fig. 9). The insignificant role of silicates for the Si concentrations is indicated by a low Al content (generally below 0·001%) in the dissolvable sediment. No analysis for Al was included in the shipboard pore water analyses (Kroenke *et al.*, 1991). Opal-A is thus progressively going into dissolution with depth. From microprobe analysis, biogenic opal-A was found to have 85–86% SiO_2 at 894 and 919 m bsf (Table 2; Fig. 10). Below 900 m bsf the concentration of silica in the pore water decreases, and the first chert nodules were noticed at 959 m bsf (Fig. 6; Kroenke *et al.*, 1991), indicating precipitation of opal-CT in line with e.g. Kastner (1979). At 1007 m bsf, Opal-CT was found as fossil-filling cement and as replacement of radiolarian remains in both cases with 94% SiO_2 (Table 2, Fig. 10). At 1098 m bsf massive silica with 98%
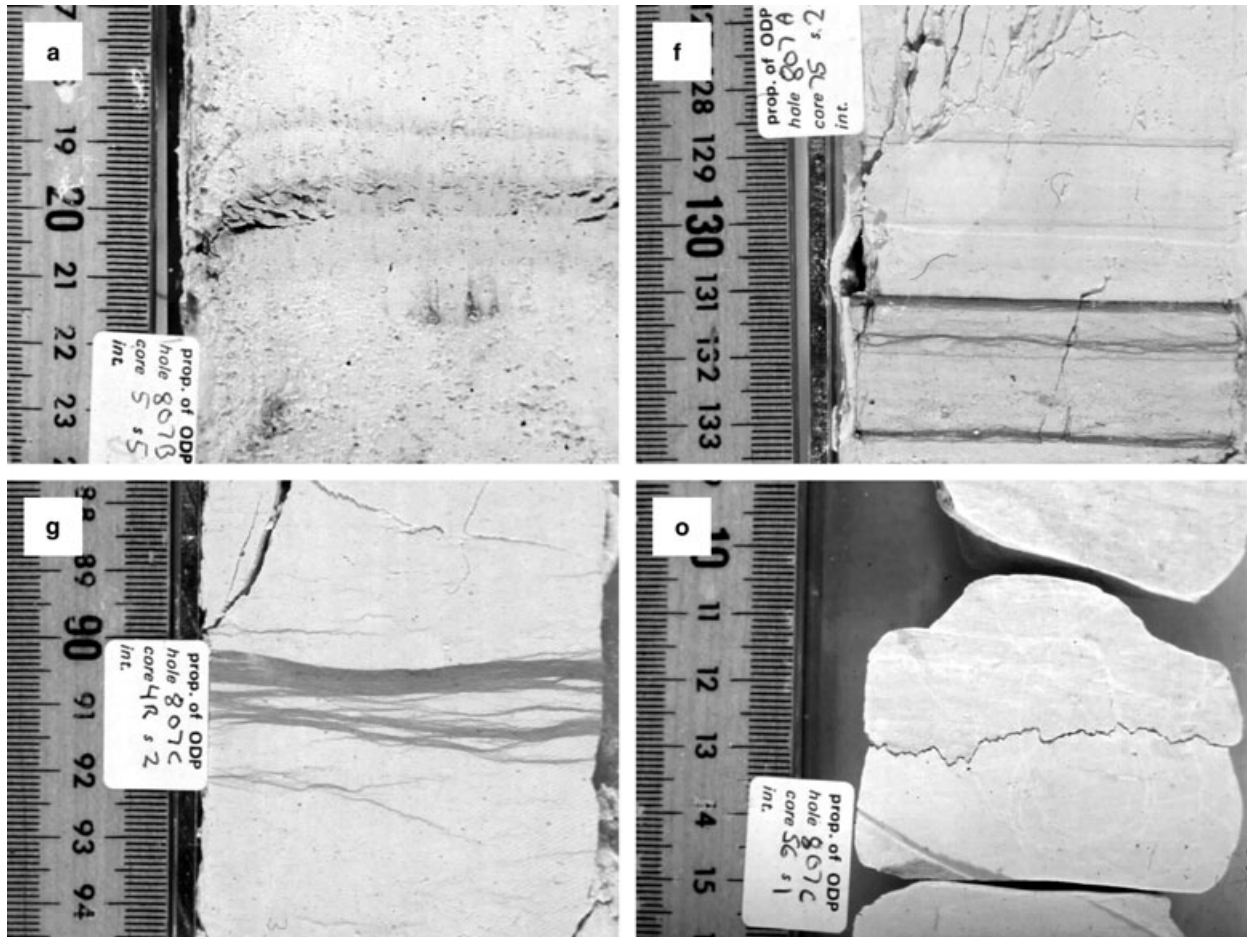
Fig. 5. Development of stylolites in Ontong Java Plateau chalk. Scale is in centimeters. (For letters refer to Fig. 4.) (a) Diffuse colour bands, 0.5 cm thick green band (darkest) with purple band (lighter) of similar thickness immediately below and a thinner purple band 0.5 cm above, 807B-5H-5; Upper Pliocene, depth: 38 m bsf, ϕ_{lab}: 67·1%. (f) Green-coloured flaser, 807A-75X-2; Lower Oligocene, depth: 710 m bsf, ϕ_{lab}: 50·9%. (g) Grey flaser, 807C-4R-2; Lower Oligocene, depth: 811 m bsf, ϕ_{lab}: 48·5%, (o) Stylolite, 807C-56R-1; Upper Maastrichtian, depth: 1207 m bsf, ϕ_{lab}: 13·1%.

SiO_2 was found (Table 2, Fig. 10). Below 1127 m bsf quartz is the only observed silica-phase, and little dissolvable Si is left in the sediment (Fig. 9).

Below the depth of onset of pore filling calcite cementation the following changes are seen in silicate mineralogy. In the interval 958–1181 m bsf clinoptilolite is found. The first occurrence of the zeolite clinoptilolite corresponds to the depth where opal-A has disappeared. From 1181 m bsf (20–25 °C) smectite-illite becomes the dominating clay mineral, and below that depth the feldspar albite is replaced by anorthite.

Sulphates and sulphides

Sulphate concentration in the pore water declines from *ca* 27 mmol l^{-1} near the sea floor to around 22 mmol l^{-1} at 350 m bsf and remains around that concentration below that depth (Kroenke *et al.*, 1991). The decline is probably partly due to sulphate-reducing bacteria giving rise to the formation of pyrite. Fe for the pyrite is partly derived from bacterially reduced magnetite (Musgrave *et al.*, 1993) and partly derived from the clay particles of the green colour bands, which may turn purple due to colouring by disseminated pyrite (Lind *et al.*, 1993). The content of dissolvable Fe in the sediment was found to be below 0·001%.

Another sink for sulphate is barite, which was noted from 191 m bsf. The barite was found as 1–10 micron size probably authigenic crystals (Fig. 11). Microprobe analysis indicates an Sr/Ba atomic ratio of around 0·03 in the barite crystals (Table 2). Sr in the pore water increases until a
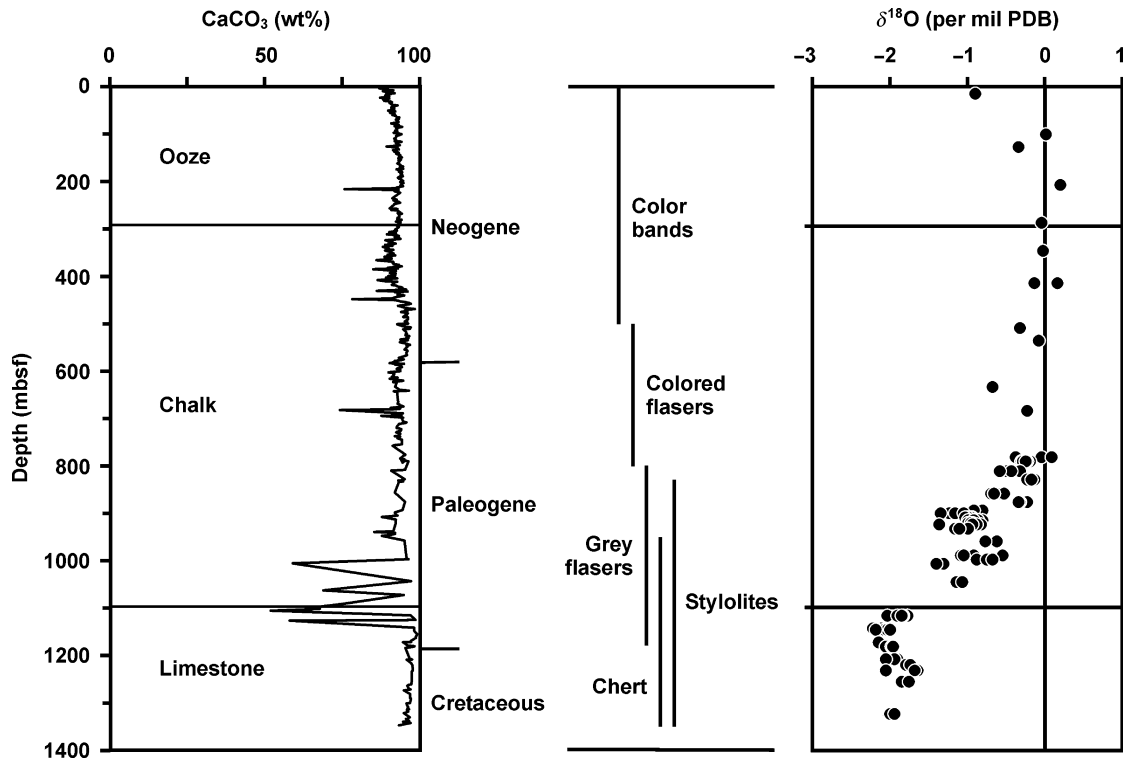
Fig. 6. Occurrence of green and purple colour bands, flaser structures, and stylolites in ODP Site 807, when compared with carbonate content in sediment (left) and $\delta^{18}O$ (right) (this study; Kroenke *et al.*, 1991; Lind, 1993a).

depth of around 200 m bsf, below which depth it gradually decreases (Fig. 9).

Texture and effect of cementation on Ontong Java Plateau and North Sea fields

Petrographic data from the OJP show how pore filling cement primarily fills the pores of microfossils (Fig. 2). Image analysis data show how the pore-filling cementation affects porosity (Fig. 4). Above the depth of onset of widespread pore-filling cementation around 1100 m bsf, large intrafossil pores and large microfossil shells contribute roughly equally to the chalk volume, so changes in bulk porosity mainly reflect changes in matrix porosity (Fig. 4). Variations in chalk texture as defined from variations in microfossil content thus only have little influence on bulk porosity in the sediments in the interval without major pore-filling cementation. The non-carbonate fraction in the ooze and chalk intervals is mainly biogenic opal.

Below 1100 m bsf pore-filling cementation is more pronounced in wackestones than in mudstones, so that the wackestone-dominated upper part of the pelagic limestone interval has markedly lower porosity than the mudstone-domin-

ated lower part of the limestone (Fig. 4). Intraclast-bearing limestone has porosity comparable with limestone with similar microtexture and no visible clasts (Fig. 4). The non-carbonate fraction is mainly diagenetic quartz which acts as a part of the pore-filling cement.

The chalk samples of Gorm and Tyra wells are less porous and more recrystallized than the Neogene and Palaeogene OJP chalk, as reflected in the lower specific surface of particles (S_{par}) in North Sea chalk than in OJP chalk (Figs 2, 4 and 12–15). The chalk of the Gorm and Tyra wells is of early Palaeogene (Danian) and Cretaceous (Maastrichtian) age and thus contemporary with the limestone of the OJP. The calcite crystals building up the chalk of Maastrichtian age in both places appear to be recrystallized to the same extent, as reflected in euhedral outline and low specific surface of particles (S_{par}) as measured by image analysis (Figs 2, 4, 12 and 14). The North Sea chalk of Danian age has higher specific surface and seems less recrystallized than the OJP limestone (Figs 2, 4 and 12–15). The chalk of Gorm and Tyra wells is significantly more porous (porosity: 20–40%) than the limestone of the OJP (porosity: 10–25%), as also reflected in a smaller specific surface of pores (S_{ϕ}) in the North Sea
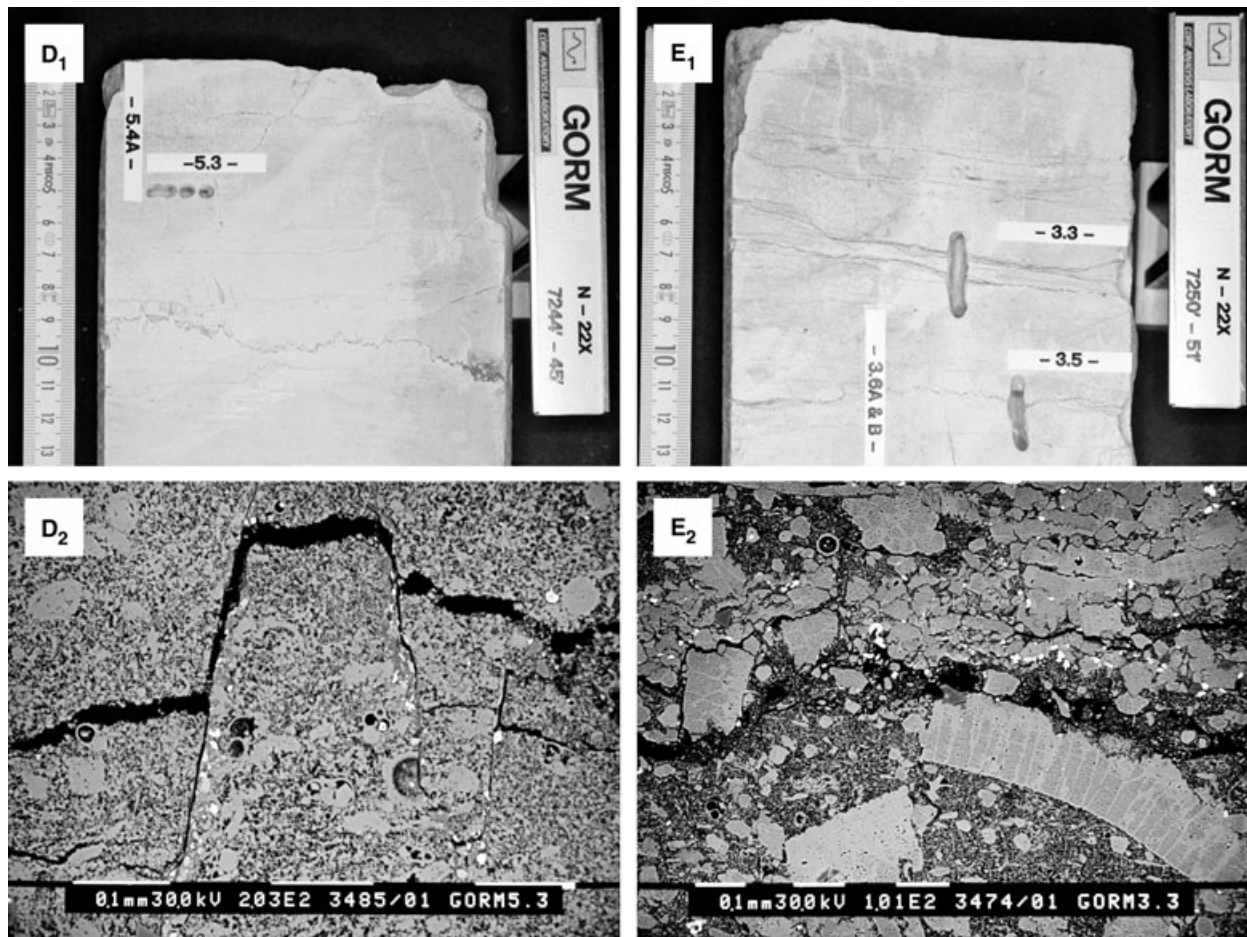
Fig. 7. Stylolites from Gorm Field. As seen in core (D_1 and E_1 – scale is in centimeters) and as seen in backscatter electron micrographs (D_2 and E_2 – scale bar is 100 microns); pyrite is white, calcite is light grey, magnesium-bearing calcite is darker grey, silicates are dark gray, and pore space is black. The near horizontal fractures are caused by sampling (for letters refer to Fig. 14). Both samples are from Upper Maastrichtian chalk in well N-22X. Sample D is from a depth of 2167 m sub sea and has a porosity of 24·6%, sample E is from a depth of 2169 m sub sea and has a porosity of 23·5%. The clay drape in both samples are dominated by kaolinite and quartz with minor amounts of pyrite, plagioclase, and barite (authigenic as well as from drilling mud) (Lind *et al.*, 1994).

chalk when compared with the OJP limestone (Figs 4, 14 and 15).

In the samples of the Gorm field, pore-filling cementation of microfossils is almost complete in chalk of Maastrichtian age, whereas in samples from Gorm and Tyra fields, cementation of microfossils is only partial in chalk of Danian age (Figs 12–15). The matrix of the Gorm Field chalk samples is recrystallized as indicated by euhedral outline of the grains, but only weakly affected by pore-filling cementation as indicated by a matrix porosity in Maastrichtian chalk of the Gorm Field being close to the matrix porosity of OJP chalk (Figs 4 and 14). In the Danian chalk samples of the Gorm and Tyra wells, pore-filling submicron-size quartz and clay reduce matrix porosity (Figs 12–15).

DISCUSSION

Stylolite formation – role of temperature and stress

Pressure dissolution at stylolites is a major source of carbonate for pore-filling cementation (e.g. Sheppard, 2002), nevertheless, it is not generally agreed whether the pressure dissolution of chalk is mainly controlled by stress at the grain contacts or by temperature dependent diffusion and precipitation (Renard *et al.*, 2000). Bjørkum (1996) and Bjørkum *et al.* (1998) interpreted petrographic data as indicating a temperature control on stylolite formation in quartzose sandstones, and supported their conclusion by referring to geochemical modeling data by Oelkers *et al.*
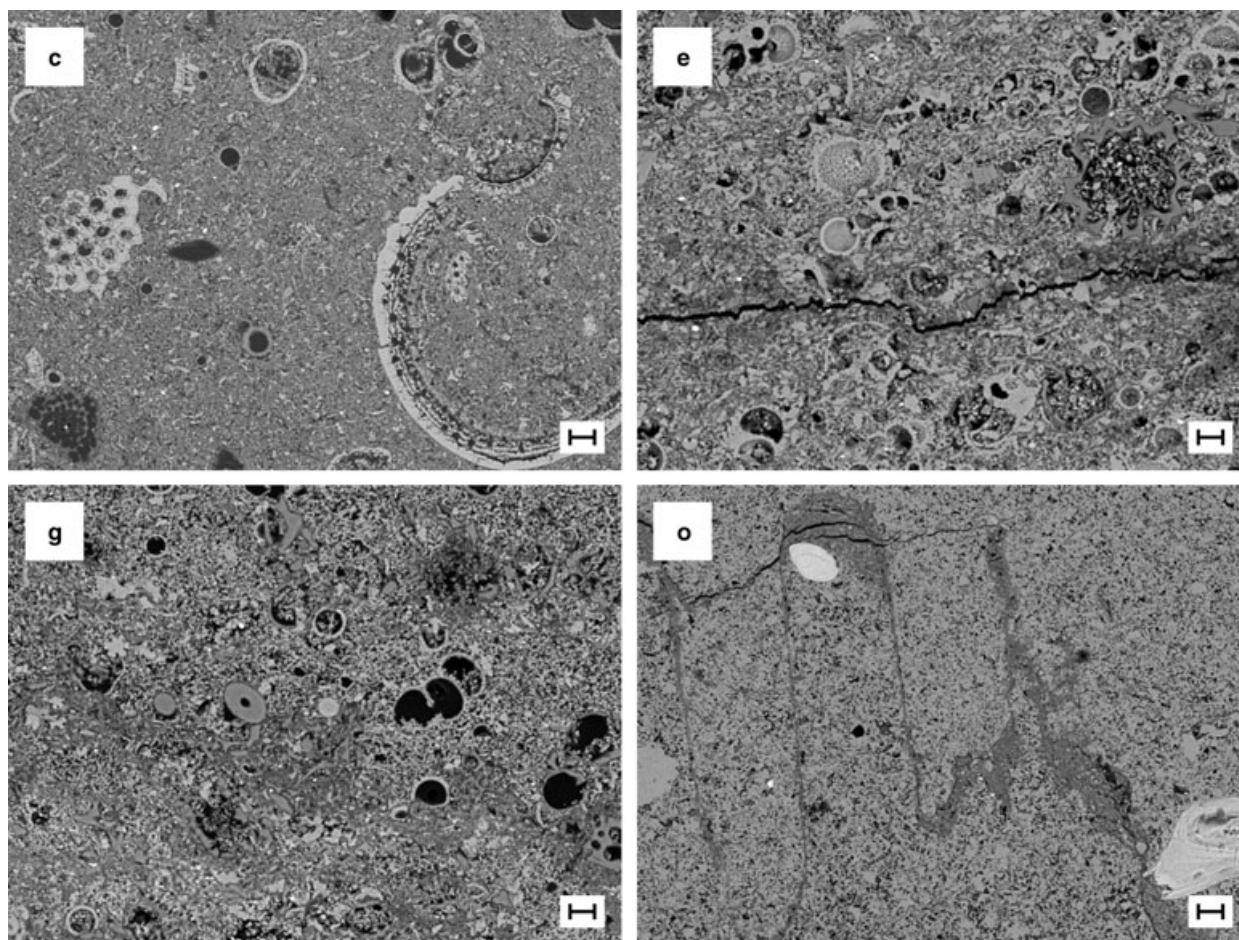
Fig. 8. Development of stylolites in Ontong Java Plateau chalk. Scale bar is 16 microns. Backscatter electron micrographs: calcite is light grey, silicates are darker grey and pore space is black. (For letters refer to Fig. 4.) (c) Diffuse colour band, 807A-12H-3; Lower Pliocene, depth: 107 m bsf, $CaCO_3$: 92·2%, ϕ_{lab}: 64·4% ϕ_{matrix}: 64·1%, non-carbonates: opal-A, chlorite-smectite, quartz, albite. (e) Coloured flaser, 807A-74X-2; Lower Oligocene, depth: 699 m bsf, $CaCO_3$: 94·4%, ϕ_{lab}: 50·6%, ϕ_{matrix}: 52·7%, non-carbonates: opal-A, smectite, quartz, albite. The near horizontal fracture is caused by sampling. (g) Grey flaser, 807C-4R-2; Lower Oligocene, depth: 811 m bsf, $CaCO_3$: 90·5, ϕ_{lab}: 48·5%, ϕ_{matrix}: 50·1%, non-carbonates: opal-CT, smectite with minor chlorite, quartz, barite, albite. (o) Stylolite, 807C-71R-2; Upper Campanian-Lower Maastrichtian, depth: 1350 m bsf, $CaCO_3$ > 62·8%, ϕ_{lab}: 23·6%, ϕ_{matrix}: 19·2%, non-carbonates: quartz, smectite-illite, anorthite. Irregular light clasts are apatitic skeletal remains.

(1992) indicating a strong temperature-dependence of quartz dissolution and precipitation rate constants as well as aqueous diffusion coefficients. Dissolution of calcite is not promoted by increasing temperature so a similar temperature dependence on stylolite formation in chalk is not to be expected.

The issue can be addressed by noting that the stylolites of the OJP resemble those of the Gorm and Tyra fields with respect to amplitude (Figs 7 and 8). The effective stress of the North Sea chalk and the stylolite-bearing chalk of the North Sea fields is similar (around 10 MPa), whereas the temperature differs. In the OJP, at 830 m bsf where stylolites start forming, the temperature is around 20 °C, at the base of the limestone at

1350 m bsf, the temperature is around 25 °C. The chalk of the Gorm and Tyra fields is at present much warmer (*ca* 70 °C), and the isotopic composition of the chalk of the Tyra Field [$\delta^{18}O$ of −4 to −2 (permil) PDB; Røgen & Fabricius, 2004] indicates that recrystallization has taken place at a higher temperature than in the OJP, where $\delta^{18}O$ generally is higher (less negative) than −2 (permil) (Fig. 6). These data thus indicate a control by stress rather than by temperature for stylolite formation in chalk.

Stylolite formation – role of sheet silicates

Whereas several authors have envisaged that stylolites develop from pressure dissolution of
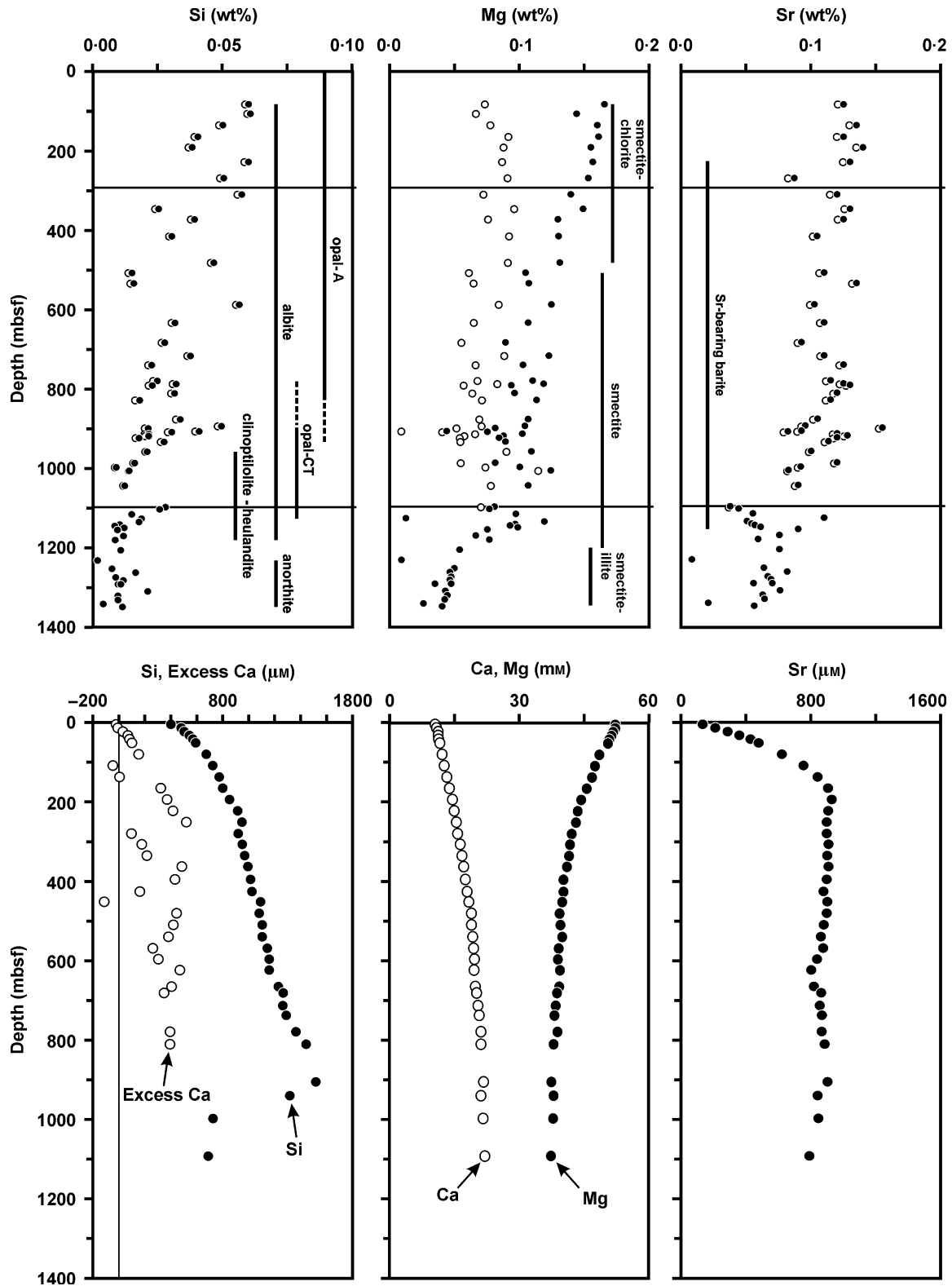
Fig. 9. ODP Site 807. Above: Concentrations of Si, Mg, and Sr in acetic acid-dissolvable part of the sediment. Solid symbols are results of analysis, open symbols are sediment composition corrected for material dissolved in pore water. The insoluble residue was analysed by X-ray diffraction, and occurrence of minerals was noted. In addition to the shown minerals most samples contain quartz. Below: concentration of Si, Mg, Ca, and Sr in pore water (Delaney *et al.*, 1991). Excess Ca in pore water was calculated by PHREEQC relative to equilibrium for calcite (Parkhurst & Appelo, 1999).
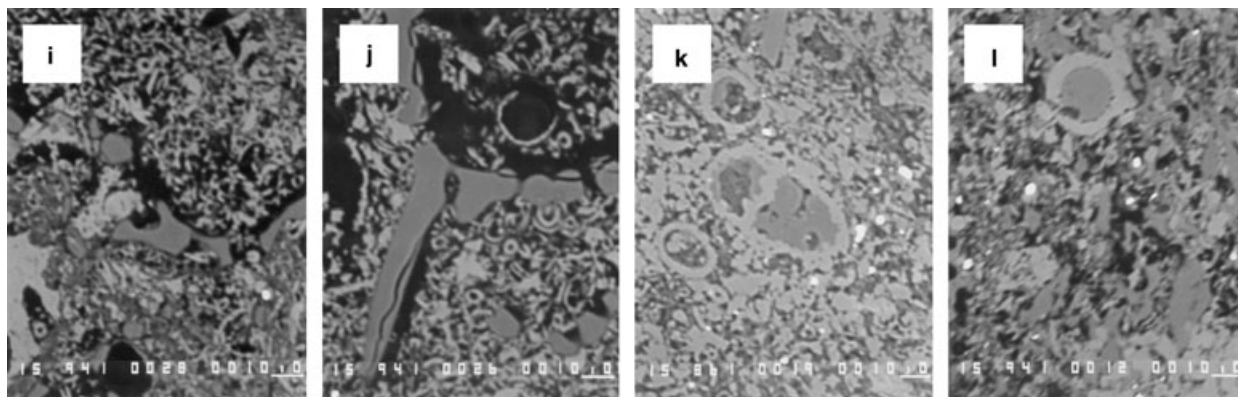
Fig. 10. Ontong Java Plateau, Leg 130, Site 807. Transition from opal to quartz. Scale bar is 10 microns. Backscatter electron micrographs: barite is white, calcite is light grey, silica is darker grey and pore space is black. (For letters refer to Fig. 4 and Table 2.) (i) Lower Oligocene, depth: 894 m bsf. Silicious fossil contains 86% SiO_2. (j) Upper Eocene, depth: 919 m bsf. Silicious fossil contains 85% SiO_2. (k) Middle Eocene, depth: 1007 m bsf. Silica contains 94% SiO_2. (l) Middle Eocene, depth: 1098 m bsf. Silica contains 98% SiO_2.
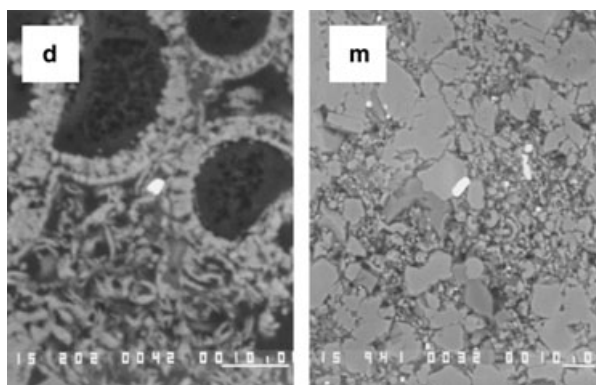

Fig. 11. Ontong Java Plateau, Leg 130, Site 807. Strontium-bearing barite. Scale bar is 10 microns. Backscatter electron micrographs: barite is white, calcite is light grey, silica is darker grey, and pore space is black. (For letters refer to Fig. 4 and Table 2.) (d) Upper Miocene, depth: 228 m bsf. Barite crystal has Sr/Ba of 0·055. (m) Lower Eocene, depth: 1127 m bsf. Barite crystals have Sr/Ba of 0·031.

calcite–calcite contacts (or quartz–quartz in sandstones) (e.g. Scholle, 1977; Bathurst, 1995; Sheldon *et al.*, 2003), petrographic evidence frequently points to a role of sheet-silicates. Heald (1955) and several later authors including Bjørkum (1996) found stylolites in sandstone to be localized at quartz–phyllosilicate contacts. Bathurst (1995) concluded that localization at phyllosilicates is not necessary for stylolite formation, and sketched three field observations showing that stylolites do not always follow bedding. Similar observations were done by Simpson (1985). In OJP stylolites may follow fractures or biogenic structures at an angle to bedding (Lind, 1993a),

but the clay drape on the stylolite may indicate that the fracture has been coated with phyllosilicates prior to stylolite formation. Safaricz & Davison (2005) studied the volumetric effect of pressure dissolution at two localities in the North Sea chalk. By assuming that the incipient stylolites were randomly distributed in chalk, they calculated a chalk sediment column shortening of around 50% and that around half the dissolved calcite was reprecipitated as cement, whereas the other half should have left the system. This would require a fluid flux so enormous (a minimum of 8000 unit volumes of fresh water per unit volume of preserved chalk in the Machar field; Safaricz & Davison, 2005), that it must be considered unrealistic. The conclusion may be that the basic assumption of a random stylolite distribution is not valid.

Baker *et al.* (1980) showed that in pressure dissolution experiments with calcite, the presence of clay prevents recrystallization of calcite. Their data indicate that the clay inhibits the precipitation of calcite, but also that clay does not retard the dissolution of calcite. This indicates that the contact between calcite and clay is a place of disequilibrium for calcite where dissolution but not precipitation is possible.

Weyl (1959) advanced the idea that pressure dissolution takes place via a thin water film in the contact between crystals. The dissolved ions should then be transported to the pores in the water film. This mechanism is simpler at a calcite–clay interface than at a calcite–calcite interface, according to the following argument: recrystallization creates a smooth interface

Table 2. Wavelength dispersive microprobe analysis data of single mineral grains.

Sample	Depth (m bsf)	Sr/Ba (atomic ratio) (average)	Sr/Ba (standard deviation)	No. of analysed particles
Barite				
807A, 25H-2, 79–81 cm (d, Figs 4 and 11)	228	0·055	0·052	3
807A, 62X-5, 7–9 cm	588	0·068	0·067	4
807C, 2R-2, 40–42 cm	792	0·033	0·018	3
807C, 31R-1, 17–19 cm	1007	0·034	0·013	4
807C, 44R-1, 30–32 cm	1116	0·030	0·003	3
807C, 45R-2, 3–5 cm (m, Figs 4 and 11)	1127	0·031	0·005	3
807C, 46R-1, 40–42 cm	1136	0·038	0·009	4
807C, 50R-1, 40–42 cm	1156	0·029	0·004	3
Silica		SiO_2 (wt%) (average)	SiO_2 (wt%) (standard deviation)	
807C, 15R-1, 33–35 cm (i, Figs 4 and 10)	894	86·0	0·6	4
807C, 20R-1, 16–18 cm (j, Figs 4 and 10)	919	85·4	0·7	4
807C, 31R-1, 17–19 cm (k, Figs 4 and 10)	1007	94·2	1·5	10
807C, 41R-1, 47–49 cm (l, Figs 4 and 10)	1098	98·0	0·4	12

where two calcite grains are held together by a strong monolayer water-bridge. Across the bridge, Ca and carbonate ions may be transported from the calcite particle in the less stable crystallographic orientation to the particle in the more stable orientation. This process does not seem to involve net dissolution of calcite or porosity loss under normal burial diagenetic conditions (Fabricius, 2003) whereas, at high stress, pressure dissolution among calcite particles is well documented (Baker *et al.*, 1980). Under normal burial diagenetic conditions, contact between calcite and clay under stress promotes dissolution because it involves forcing the calcite into the ion exchange layer of the clay. Ca ions can thus be transported from the solid interface to the solution via an ion exchange conveyer belt. This approach is largely similar to the conclusion of Renard & Ortoleva (1997), who pointed to thick fluid layers at sheet silicates, giving rise to easier diffusion. Stylolites thus tend to be localized at clay, because the cation exchange capacity of the clay furthers dissolution and counteracts precipitation at the interface.

Recrystallization

The mineralogical constituents of the OJP sediments and sedimentary rocks equilibrate with pore water as a function of temperature and time, and equilibration of one mineral influences the other. These processes are not directly influencing porosity, but may facilitate mechanical compaction by smoothing particles (Borre &

Fabricius, 1998) and influence the transport of ions dissolved at stylolites.

During recrystallization, calcite releases Sr (Baker *et al.*, 1982; Delaney & Linn, 1993) and approaches stable crystal shape, a process which is largely over for sediments of Palaeogene age (Figs 4, 6 and 9). The released Sr precipitates as a component in barite (Fig. 11) and because it gets trapped in insoluble barite a general depthwise fall in content of dissolvable Sr in the sediment is seen (Fig. 9). Delaney & Linn (1993) suggested that the formation of celestite could explain the concurrent decline in sulphate and stabilization of Sr in the pore water, but no celestite was observed in the present study, so at least the main part of the dissolved Sr is taken up by barite. Cronan (1974) cited authors reporting up to 3% Sr in solid solution in microcrystalline barite in deep-sea sediments. A diagenetic origin of barite at this pelagic site is in accordance with the observations of Von Breymann *et al.* (1989) and Dymond *et al.* (1992). Ba is probably released during decay of organic matter from siliceous fossils (Bishop, 1988), in the present case taking place during sulphate reduction. A hydrothermal source of Ba and Sr is hardly likely in the geological setting on the OJP.

The siliceous fossils (radiolarians and diatoms) originate as opal-A, but are gradually dissolved, as indicated by etched outline (Fig. 10i,j), and reprecipitated as opal-CT which develops into quartz (Figs 9 and 10k,l). Based on a compilation of data from 37 DSDP volumes of rates and temperature of formation of opal-
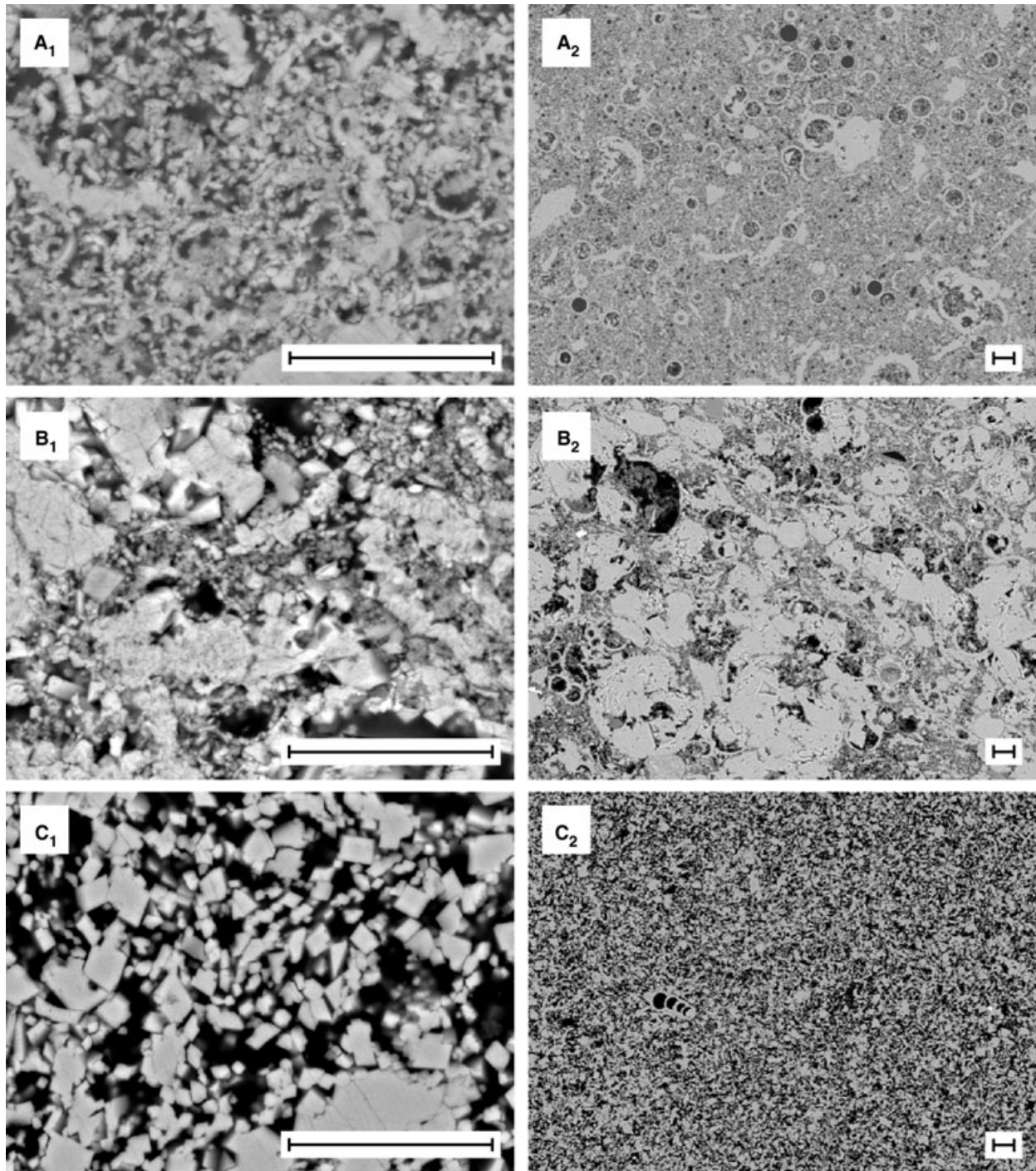
Fig. 12. North Sea, Gorm Field, Well N-22X. Scale bar is 16 microns. Texture and carbonate content control porosity and degree of recrystallization. The fine-grained non-carbonates include quartz and kaolinite. Backscatter electron micrographs: calcite is light grey, silicates are darker grey and pore space is black. (For letters refer to Fig. 14.) (A) N-22X; Danian, depth: 2093·1 m sub sea, $CaCO_3$: 84·5%, ϕ_{lab}: 30·2%, ϕ_{matrix}: 45·9%. The silicate rich wackestone has high porosity and relatively low recrystallization of matrix particles. Silicates generally occur as submicron size particles. (B) N-22X; Danian, depth: 2114·0 m sub sea, $CaCO_3$: 89·6%, ϕ_{lab}:23·1%, ϕ_{matrix}: 39·2%. The poorly sorted chalk packstone has low porosity. Microfossils tend to be cemented and silicates generally occur as submicron size particles. (C) N-22X; Maastrichtian, depth: 2127·1 m sub sea, $CaCO_3$: 98·2%, ϕ_{lab}:36·0%, ϕ_{matrix}: 49·5%. The well-sorted chalk mudstone has high porosity. A high degree of recrystallization is indicated by the equant calcite crystals of the chalk matrix (C_1).
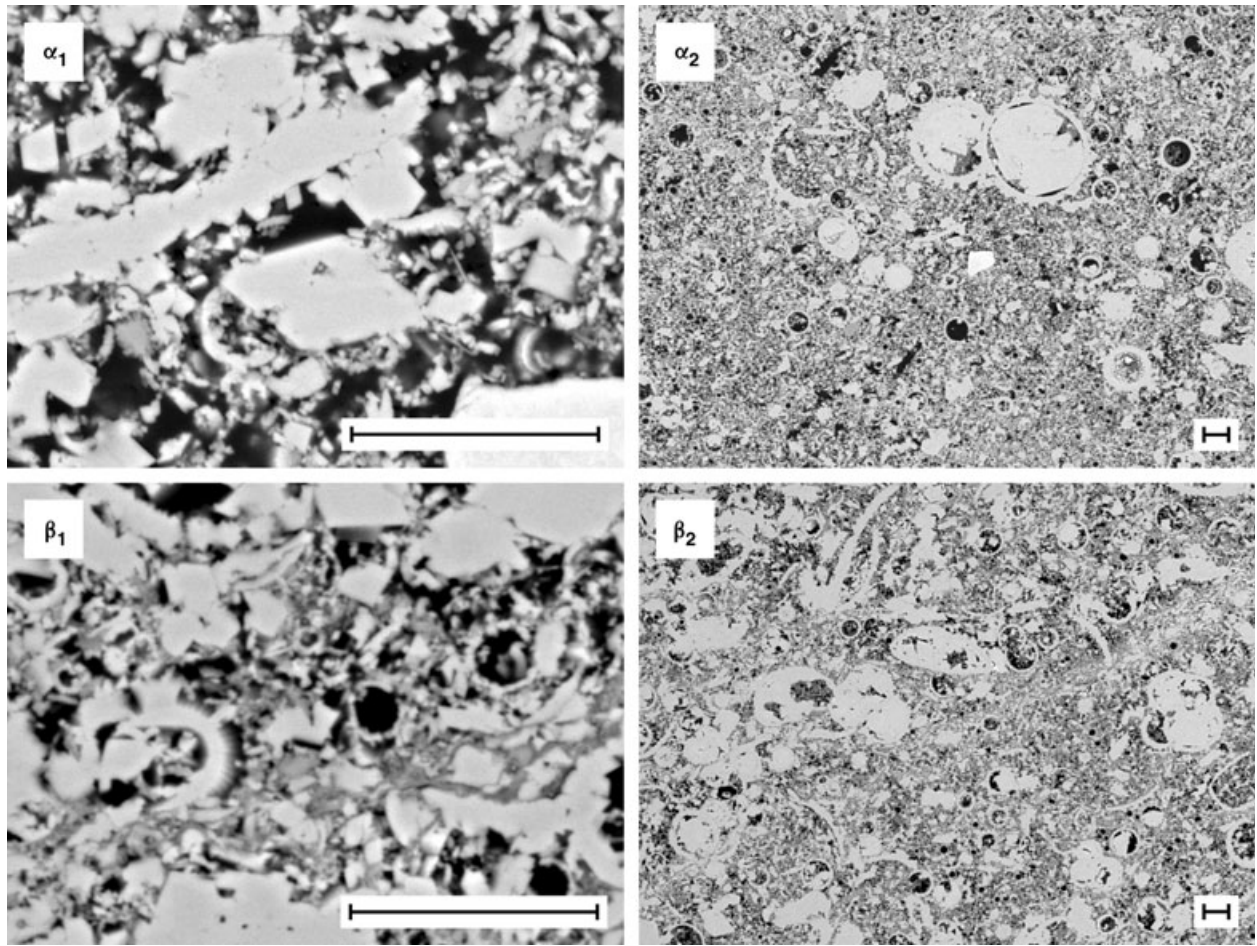
Fig. 13. North Sea, Tyra Field, Well E-5X. Scale bar is 16 microns. Porosity is controlled by content of microfossils and content of carbonate. The non-carbonates include quartz and smectite. Backscatter electron micrographs: calcite is light grey, silicates are darker grey and pore space is black. (For letters refer to Fig. 15.) (α) E-5X; Danian, depth: 2019·9 m sub sea, $CaCO_3$: 94·5%, ϕ_{lab}: 33·6%, ϕ_{matrix}: 36·4%. The relatively pure and well-sorted chalk has high porosity. (β) E-5X; Danian, depth: 2027·0 m sub sea, $CaCO_3$: 86·7%, ϕ_{lab}: 21·8%, ϕ_{matrix}: 29·2%. The relatively impure and poorly sorted chalk has low porosity. A stylolite transects the image from lower left to upper right. The drape is composed mainly of smectite and quartz.

CT, the following relationship was found by Kastner (1979):

$$t = 80 - 2T + 0·01T^2 \qquad (1)$$

$$t = 83 - 4·15T + 0·1T^2 - 0·001T^3 \qquad (2)$$

where t is time after deposition in millions of years and T is present day temperature (°C). Eq. 1 represents slower sedimentation rates and/or lower geothermal gradients and/or less carbonate-rich sediments than Eq. 2. According to Eq. 2, 31–43 Ma corresponds to 13–21 °C in accordance with the present data. The transformation from opal-CT to quartz is accompanied by a drop in Si concentration in the pore water, which may also be influenced by precipitation of clinoptilolite-heulandite (Fig. 9).

The mineralogical recrystallization will also to some extent modify sedimentary structures.

Fig. 14. Data from well N-22X in Gorm Field. Porosity is from He-porosimetry on discrete samples (dots) and calculated from the density log (solid line). Composition is from analysis of BSE-images. Signatures from left to right indicate: light grey: silicates, white: large particles or large cemented area, hatched: small particles, dark gray: large porosity, medium grey: small porosity (Figs 3 and 12). Matrix porosity is from image analysis (Figs 3 and 12). BET is specific surface as measured by N_2 adsorption. S_{par} and S_ϕ are specific surface as measured by image analysis with reference to particles, respectively with reference to porosity.
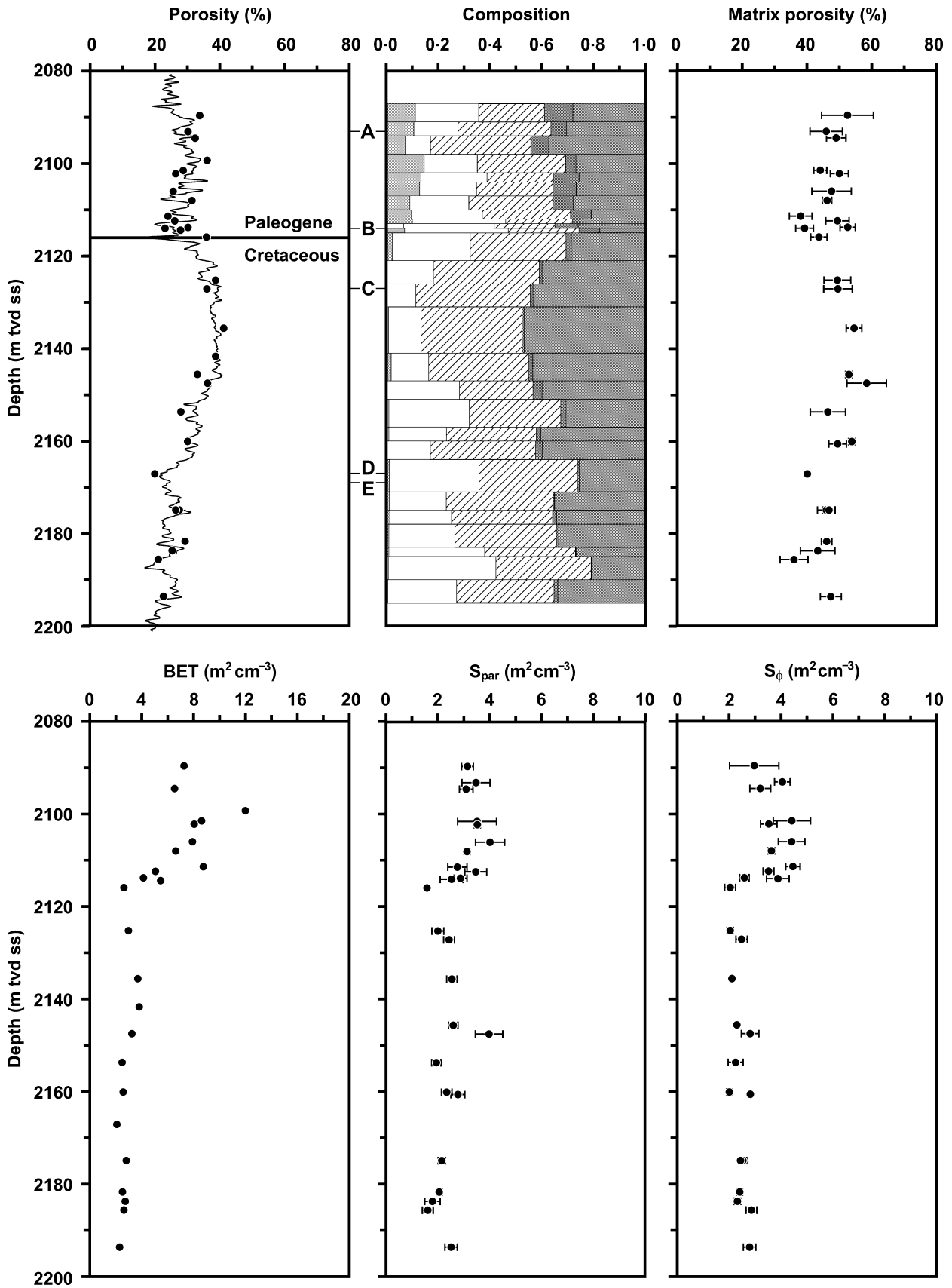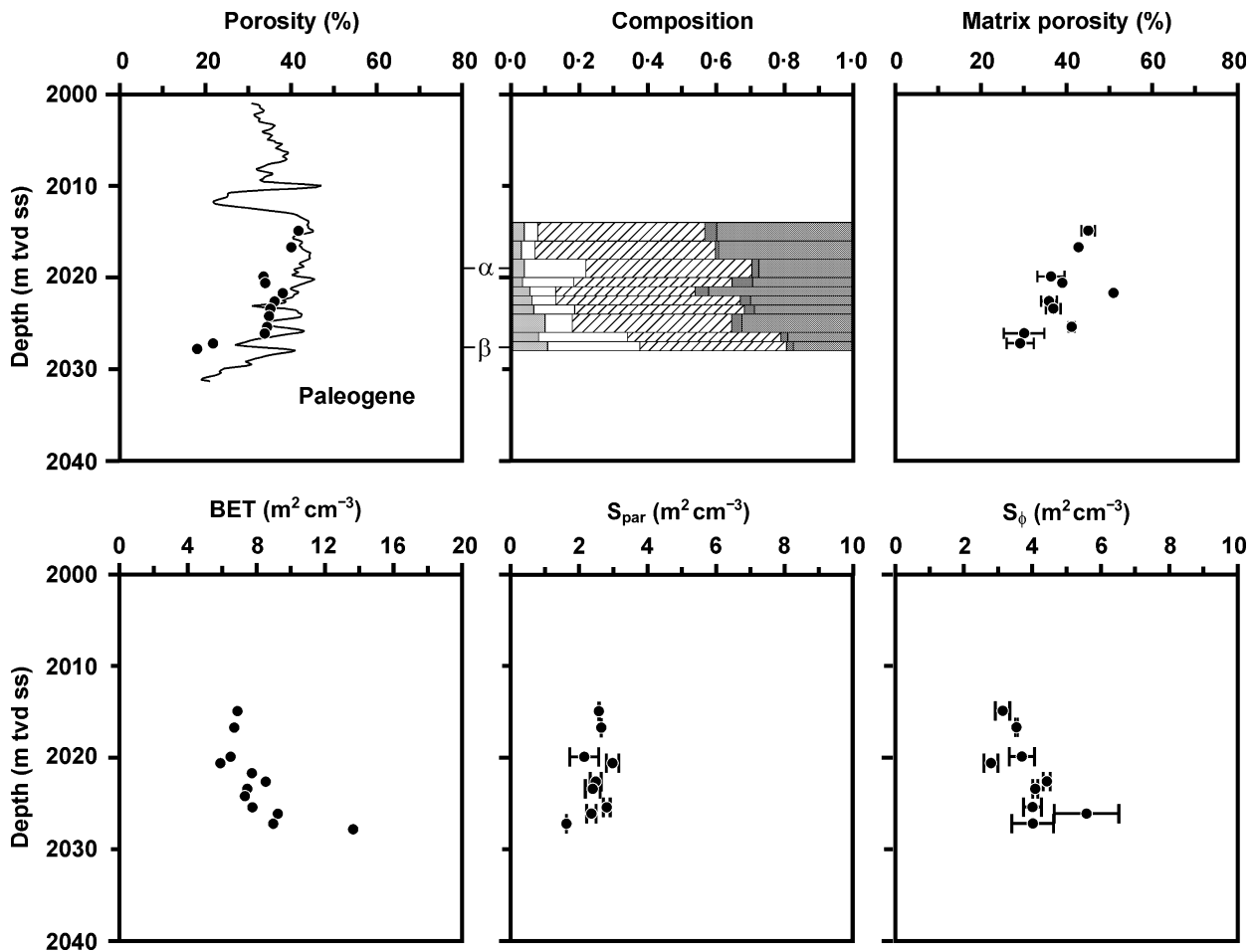
Fig. 15. Data from well E-5X in Tyra Field. Porosity is from He-porosimetry on discrete samples (dots) and calculated from the density log (solid line). Composition is from analysis of BSE-images. Signatures from left to right indicate; light grey: silicates, white: large particles or large cemented area, hatched: small particles, dark gray: large porosity, medium grey: small porosity (Figs 3 and 13). Matrix porosity is from image analysis (Figs 3 and 13). BET is specific surface as measured by N_2 adsorption. S_{par} and S_{ϕ} are specific surface as measured by image analysis with reference to particles, respectively with reference to porosity.

Green colour bands contain smectite-chlorite, whereas coloured flasers contain smectite (Figs 6 and 9). In order to form the wispy structure, the clay minerals must have recrystallized, while releasing Fe. Mg in pore water decreases with depth at a declining rate, and thus probably not only reflects diffusion of Mg from sea water to basement but also reflects uptake of Mg during this recrystallization, although a corresponding increase in sediment Mg-content is less obvious (Fig. 9). The transition from opal-A to opal-CT accompanies the development of grey flaser structures and stylolites as well as initial pore-filling calcite-cementation, and the transition from opal-CT to quartz accompanies the marked increase in pore-filling calcite-cementation below 1100 m bsf.

Calcite cementation – role of silica

Changes in silica-modification seem to influence calcite cementation. A control of calcite cementation by silica was also reported by Hobert & Wetzel (1989). They studied deep-sea carbonates and found 'carbonate sediments containing chert (1) tend to be more indurated and display more advanced diagenetic alteration, regardless of sub-bottom depth'. Correspondingly, Baker *et al.* (1980) found that diatoms inhibit calcite recrystallization.

The opal-A of diatoms and radiolarians will cause a relatively high concentration of Si in the pore water, which will counteract carbonate cement precipitation for the following reason: Tanaka & Takahashi (2000, 2002) found that

whereas all alkali and earth-alkali metal ions facilitate dissolution of silica, Sr, Ca, and Na ions form stable complexes with silicate ions in chloride solutions comparable to sea water. Ca and especially Sr ions form more stable complexes than Na ions, so although the pore water of ODP Site 807 contains $0{\cdot}5$ mol l^{-1} Na (Delaney *et al.*, 1991), the concentration of Ca is high enough (>10 mmol l^{-1}, Fig. 9) for Ca–silicate complexes to dominate. Sr concentrations are too low to be significant in this context (Fig. 9). Fabricius (2003) found that the pore water of ODP Site 807 is supersaturated with respect to calcite and explained it by adsorbed Mg-ions acting as a shield of Mg-calcite according to Neugebauer (1974) and Berner (1975). No Mg-calcite was observed, so in this case a more simple explanation for the apparent Ca-supersaturation is the formation of Ca–silicate complexes in the pore water. The Si-concentration in the pore water is indeed 2–4 times that of the excess Ca (Fig. 9), allowing all excess Ca to be part of silica complexes. When opal-A is the dominating silica-phase, the pore water will be so rich in Si that a part of the Ca released during recrystallization and Ca generated by pressure dissolution will not precipitate, but rather form Si-complexes in the pore water or take part in the overall diffusion of Ca from basement to sea water. No net calcite cementation was seen before silica in the pore water starts falling as a consequence of opal-CT formation and a conspicuous calcium cementation front is seen when opal-CT has been replaced by quartz. Calcite cementation is thus probably controlled by the diagenetic development of silica phases and thus temperature, and the frequently reported apparent supersaturation of Ca in pore water in carbonate sediments may be a consequence of not taking Ca–silica complexes into account in geochemical calculations.

Calcite cementation and porosity – role of depositional texture

Down to the cementation front in the OJP, variations in primary texture have little influence on total porosity, but in the deep cemented interval the influence of primary texture on porosity is significant (Fig. 4). Because microfossils are preferentially filled with cement, wackestones get lower porosity than mudstones. This is the explanation for the reversing porosity trend in the deepest part of ODP Site 807 (Fig. 4). The microfossil-rich interval thus has lower porosity than the underlying mudstones. Due to

their relatively high porosity, the mudstones cannot have formed by a gradual depth-wise disappearance of foraminifers due to preferential dissolution and precipitation, as suggested by Schlanger & Douglas (1974), but must rather be seen as having primary texture.

Petrographic image analysis indicates that the local porosity variations in the Gorm and Tyra fields are also due to differences in primary sediment composition. Low porosity may be caused by a high content of cemented microfossils or by a high content of pore-filling silicates. A combination of the two effects causes particularly low porosity in the lower part of the Danian section as seen in the data of the Tyra Field (Figs 13, 15).

Comparison of porosity and permeability, Ontong Java Plateau and North Sea fields

The porosity of the chalk of Gorm and Tyra fields has a different textural distribution compared with OJP chalk and limestone. Gorm and Tyra chalk is similar to OJP limestone by having cemented microfossils, but differs in having larger matrix porosity and less pore-filling cementation of matrix (Figs 4, 14 and 15). Gorm and Tyra chalk is similar to OJP chalk with respect to matrix porosity but differs by having cemented microfossils (Figs 4, 14 and 15).

The similar matrix porosity may be a reflection of the similar degree of (now arrested) mechanical compaction. The mechanical compaction of OJP seems to have arrested around 600 m bsf, below which depth sediment stiffening and increase in particle and pore size take place by internal redistribution of calcite (recrystallization), before the onset of pore-filling cementation (Fabricius, 2003). A similar arrest in mechanical compaction and subsequent pore-growth may have taken place in the North Sea fields before their present effective burial as indicated by a relatively high sonic P-wave velocity (Borre, 1998).

In spite of the relatively large pores and large porosity of the OJP, the permeability is probably lower than in the North Sea chalk (Fig. 16). The reason is the relatively high specific surface as measured by BET (Figs 4, 14 and 15). The difference in BET is caused by the content of opal in the OJP chalk, whereas quartz is the only reported silica phase in the studied Gorm and Tyra chalk (Lind *et al.*, 1994; Røgen & Fabricius, 2002).

The lack of pore-filling inter-particle cementation in the matrix of the chalk of the Gorm and
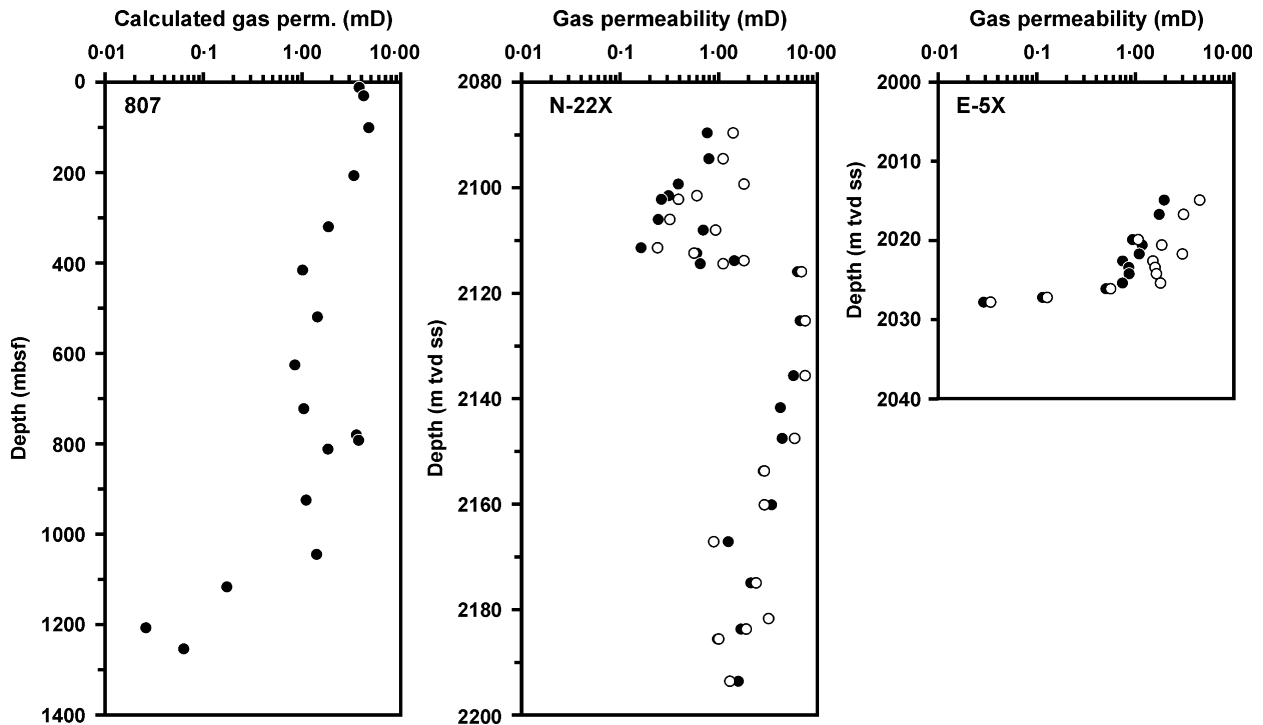
Fig. 16. Permeability of studied samples. Measured gas permeability is open circles. Black symbols represent permeability calculated from Kozeny's equation and a relationship between gas permeability and liquid permeability as given in Mortensen *et al.* (1998).

Tyra fields indicates a more gradual cementation when compared with the OJP, where a cementation front is seen. The differences may be explained in several ways:

1 The introduction of hydrocarbons into the two North Sea structures may have impeded pore-filling cementation at a critical initial stage of cementation, only allowing volume-preserving recrystallization of matrix crystals, but, however, allowing cement precipitation within the water-filled microfossils.

2 The cementation in the OJP may be promoted by Ca^{2+} diffusing from the basaltic basement, whereas the chalk of Gorm and Tyra probably only has calcite dissolved at stylolites as a source of pore filling cement.

3 The difference in burial history and temperature between central North Sea and OJP. In the studied North Sea fields, overpressure has lowered the rate of effective burial, and hence caused a low effective burial relative to temperature. The silica of the North Sea chalk may originate from opal that has recrystallized to quartz at a stage where compaction was not completed and stylolites had not started forming. The sudden cementation caused by the drop in silica in the pore water of the deep-sea chalk may thus not

have taken place in the studied North Sea chalk wells.

In the cold Ontong Java Plateau net dissolution of calcite is controlled by stress whereas net precipitation is controlled by temperature. In the warmer chalk of the central North Sea dissolution as well as precipitation may be stress controlled because of relatively early transformation from opal to quartz. When exploring for hydrocarbons in normally pressured chalk, experience with respect to porosity-development from overpressured chalk thus cannot be directly applied.

CONCLUSIONS

Stylolite formation is a major agent of calcite dissolution causing calcite-cementation in chalk. Stylolites have similar size in the chalk of the Ontong Java Plateau and in the chalk of the Gorm and Tyra fields of the central North Sea, where effective stress is similar but temperature differs. These observations indicate that stylolite formation is controlled by effective stress.

Stylolites tend to be localized at clay, probably because pressure dissolution is promoted where

calcite is squeezed into the electric double layer of clay with cation exchange capacity, so that ions may be conveyed away from the point of contact. In addition the presence of clay counteracts precipitation of calcite.

In the Ontong Java Plateau the stylolites originiate in green colour bands containing smectite-chlorite and opal-A, which upon burial recrystallize to smectite- and opal-A-bearing green flaser structures, where the first signs of pressure dissolution are seen. Upon further burial they recrystallize into smectite- and opal-CT-bearing grey flaser structures and stylolites, which deeper down are replaced by quartz- and illite-smectite-bearing stylolites.

Whereas net dissolution of calcite is controlled by stress at stylolites, calcite precipitation in the Ontong Java Plateau is probably controlled by temperature. The reason is that silica-diagenesis controls the amount of Si in the pore water, and Ca–silicate complexes in the pore water may cause apparent super-saturation with calcite. When opal is transformed to quartz due to increasing temperature, the silica content in the pore water declines, and calcite precipitates as a cementation front.

In the Ontong Java Plateau, above the cementation front, variations in primary texture have little influence on total porosity but, in the deep cemented interval, wackestone has lower porosity than mudstone due to preferential cementation of microfossils.

In the central North Sea Gorm and Tyra fields, overpressuring is reflected in a relatively low effective stress for a given depth and consequently a high ratio between temperature and effective stress. This has probably caused silica transformation to quartz before the onset of stylolite formation and consequent direct calcite cementation. The chalk is partly cemented as reflected in cemented microfossils and a porous matrix, apparently with little pore-filling cement.

Burial stress and temperature thus play distinct roles in burial diagenesis and porosity-development of chalk. Burial stress controls physical compaction and pressure dissolution, whereas temperature controls recrystallization and cementation.

ACKNOWLEDGEMENTS

REFERENCES

Bachman, R.T. (1984) Intratest porosity in foraminifera. *J. Sed. Petrol.*, **54**, 257–262.

Baker, P.A., Kastner, M., Byerlee, J.D. and **Lockner, D.A.** (1980) Pressure dissolution and hydrothermal recrystallization of carbonate sediments – an experimental study. *Mar. Geol.*, **38**, 185–203.

Baker, P.A., Gieskes, J.M. and **Elderfield, H.** (1982) Diagenesis of carbonates in deep-sea sediments – evidence from Sr/Ca ratios and interstitial dissolved Sr^{2+} data. *J. Sed. Petrol.*, **52**, 71–82.

Bathurst, R.G.C. (1995) Burial diagenesis of limestones under simple overburden. Stylolites, cementation and feedback. *Bull. Soc. Geol. Fr.*, **166**, 181–192.

Berger, W.H. and **Lind, I.L.** (1997) Abundance of color bands in Neogene carbonate sediments on Ontong Java Plateau: a proxy for sedimentation rate. *Mar. Geol.*, **144**, 1–8.

Berner, R.A. (1975) The role of magnesium in the crystal growth of calcite and aragonite from sea water. *Geochim. Cosmochim. Acta*, **39**, 489–504.

Bishop, J.K.B. (1988) The barite-opal-organic carbon association in oceanic particulate matter. *Nature*, **332**, 341–343.

Bjørkum, P.A. (1996) How important is pressure in causing dissolution of quartz in sandstones? *J. Sed. Res.*, **A66**, 147–154.

Bjørkum, P.A., Oelkers, E.H., Nadeau, P.H., Walderhaug, O. and **Murphy, W.M.** (1998) Porosity prediction in quartzose sandstones as a function of time, temperature, depth, stylolite frequency, and hydrocarbon saturation. *AAPG Bull.*, **82**, 637–648.

Borre, M. (1997) Porosity variation in Cenozoic and Upper Cretaceous Chalk from the Ontong Java Plateau – a discussion of image analysis data. In: *Research in Petroleum Technology* (Ed. M.F. Middleton), pp. 1–15. Nordic Petroleum Series 3, Ås Norway.

Borre, M. (1998) Ultrasonic velocity of North Sea Chalk – predicting saturate data from dry. In: *Research in Petroleum Technology* (Ed. M.F. Middleton). pp. 71–98. Nordic Petroleum Series, 4, Ås Norway.

Borre, M. and **Fabricius, I.L.** (1998) Chemical and mechanical processes during burial diagenesis of chalk. An interpretation based on specific surface data of deep-sea sediments. *Sedimentology*, **45**, 755–770.

Borre, M., Lind, I. and **Mortensen, J.** (1997) Specific surface as a measure of Burial Diagenesis of Chalk. *Zbl. Geol. Paläont. Teil 1*, **1995**, 1071–1078.

Cronan, D.S. (1974) Authigenic minerals in deep-sea sediments. In: *The Sea, 5* (Ed. E.D. Goldberg), pp. 491–525. John Wiley & Sons, New York.

Delaney, M.L. and Linn, L.J. (1993) Interstitial water and bulk calcite chemistry, Leg 130, and calcite recrystallization. *Proc. ODP Sci. Results*, 130, 561–572.

Delaney, M.L. and Shipboard Scientific Party (1991) Inorganic geochemistry summary. *Proc. ODP Init. Rep.*, 130, 549–551.

Doyle, M.C. and Conlin, J.M. (1990) The Tyra Field. In: *North Sea Oil and Gas Reservoirs II* (Eds A.T. Buller, E. Berg, O. Hjelmeland, J. Kleppe, O. Torsæter and J.O. Aasen), pp. 47–65. Graham & Trotman, London.

Dymond, J., Suess, E. and Lyle, M. (1992) Barium in deep-sea sediment: a geochemical proxy for paleoproductivity. *Paleoceanography*, 7, 163–181.

Fabricius, I.L. (2003) How burial diagenesis of chalk sediments controls sonic velocity and porosity. *AAPG Bull.*, 87, 1755–1778.

Heald, M.T. (1955) Stylolites in sandstone. *J. Geol.*, 63, 101–114.

Hobert, L.A. and Wetzel, A. (1989) On the relationship between silica and carbonate diagenesis in deep-sea sediments. *Geol. Rundsch.*, 78, 765–778.

Hurst, C. (1983) Petroleum geology of the Gorm field, Danish North Sea. *Geol. Mijnbouw*, 62, 157–168.

Japsen, P. (1998) Regional velocity-depth anomalies, North Sea Chalk: a record of overpressure and neogene uplift and erosion. *AAPG Bull.*, 82, 2031–2074.

Jensenius, J. (1987) High-temperature diagenesis in shallow Chalk reservoir, Skjold oil field, Danish North Sea: evidence from fluid inclusions and oxygen isotopes. *AAPG Bull.*, 71, 1378–1386.

Kastner, M. (1979) Authigenic silicates in deep-sea sediments: formation and diagenesis. In: *The Sea 7* (Ed. C. Emiliani), pp. 915–980. John Wiley & Sons, New York.

Krissek, L.A. and Janecek, T.R. (1993) Eolian deposition on the Ontong Java Plateau since the Oligocene: unmixing the record of multiple dust sources. *Proc. ODP Sci. Results*, 130, 471–490.

Kroenke, L.W., Berger, W.H., Janecek, T.R. *et al.* (1991) *Proc. ODP Init. Rep.*, 130, 1240 pp.

Lind, I.L. (1993a) Stylolites in chalk from Leg 130, Ontong Java Plateau. *Proc. ODP Sci. Results*, 130, 445–451.

Lind, I.L. (1993b) Loading experiments on carbonate ooze and chalk from Leg 130, Ontong Java Plateau. *Proc. ODP Sci. Results*, 130, 673–686.

Lind, I.L., Janecek, T., Krissek, L., Prentice, M. and Stax, R. (1993) Color bands in Ontong Java Plateau carbonate oozes and chalks. *Proc. ODP Sci. Results*, 130, 453–470.

Lind, I., Nykjær, O., Priisholm, S. and Springer, N. (1994) Permeability of stylolite-bearing chalk. *J. Petrol. Technol.*, 46, 986–993.

Mahoney, J.J., Fitton, J.G., Wallace, P.J. *et al.* (2001) *Proc. ODP Init. Rep.*, 192, CD-ROM.

Mazzullo, J., Meyer, A. and Kidd, R. (1988) New sediment classification scheme for the Ocean Drilling Program. In: *Handbook for Shipboard Sedimentologists* (Eds J. Mazzullo and A.G. Graham) *Texas A&M University, Ocean Drilling Program, Technical Note*, 8, 45–67.

Moberly, R., Schlanger, S.O. et al. (1986) *Init. Rep. DSDP, 89.* US Govt. Printing Office, Washington, DC. 678 pp.

Mortensen, J., Engstrøm, F. and Lind, I. (1998) The relation among porosity, permeability, and specific surface of chalk from the Gorm field, Danish North Sea. *SPE Reservoir Eval. Eng.*, 1, 245–251.

Musgrave, R.J., Delaney, M.L., Stax, R. and Tarduno, J.A. (1993) Magnetic diagenesis, organic input, interstitial water chemistry, and paleomagnetic record of the carbonate sequence of the Ontong Java Plateau. *Proc. ODP Sci. Results*, 130, 527–546.

Neugebauer, J. (1974) Some aspects of cementation in chalk. In: *Pelagic Sediments: On Land and Under the Sea* (Eds K.J. Hsü and H.C. Jenkyns), *Int. Assoc. Sedimentol. Spec. Publ.*, 1, 149–176.

Oelkers, E.H., Bjørkum, P.A. and Murphy, W.M. (1992) The mechanism of porosity reduction, stylolite development and quartz cementation in North Sea sanstones. In: *Water-Rock Interaction 2* (Eds Y.K. Kharaka and A.S. Maest), pp. 1183–1186. Balkema, Rotterdam.

Olsen, C. (2002) Texturel tolkning af Nordsøkalks elasticitet og porekollaps. MSc Thesis, Technical University of Denmark, Lyngby.

Parkhurst, D.L. and Appelo, C.A.J. (1999) *User's Guide to PHREEQC (version 2) – a Computer Program for Speciation, Batch-Reaction, One-Dimensional Transport, and Inverse Geochemical Calculations*. U.S. Geol. Surv. Water Resour. Inv. Rep. 99-4259, 312 pp.

Røgen, B. (2002) North Sea chalk – textural, petrophysical, and acoustic properties. PhD Thesis, Environment & Resources DTU, Technical University of Denmark, Kgs. Lyngby. 106 pp.

Røgen, B. and Fabricius, I.L. (2002) Influence of clay and silica on permeability and capillary entry pressure of chalk reservoirs in the North Sea. *Petrol. Geosci.*, 8, 287–293.

Røgen, B. and Fabricius, I.L. (2004) Diagenetic ripening of six North Sea chalk fields. P334. In: *Sharing the Earth. 66th EAGE Conference and Exhibition*, Paris, 7–20 June, 2004. Extended abstracts and exhibitors' catalogue. CD-ROM, European Association of Geoscientists and Engineers, DB Houten, NL, p. 4.

Røgen, B., Gommesen, L. and Fabricius, I.L. (2001) Grain size distributions of Chalk from image analysis of electron micrographs. *Comput. Geosci.*, 27, 1071–1080.

Renard, F. and Ortoleva, P. (1997) Water films at grain-grain contacts: Debye-Huckel, osmotic model of stress, salinity and mineralogy dependence. *Geochim. Cosmochim. Acta*, 61, 1963–1970.

Renard, F., Brosse, E. and Gratier, J.P. (2000) The different processes involved in the mechanism of pressure solution in quartz-rich rocks and their interactions. In: *Quartz Cementation in Sandstones* (Eds R.H. Worden and S. Morad), *Int. Assoc. Sedimentol. Spec. Publ.*, 29, 67–78.

Safaricz, M. and Davison, I. (2005) Pressure solution in chalk. *AAPG Bull.*, 89, 383–401.

Schlanger, S.O. and Douglas, R.G. (1974) The pelagic ooze-chalk-limestone transition and its implications for marine stratigraphy. In: *Pelagic Sediments: On Land and Under the Sea* (Eds K.J. Hsü and H.C. Jenkyns). *Int. Assoc. Sedimentol. Spec. Publ.*, 1, 117–148.

Scholle, P.A. (1977) Chalk diagenesis and its relation to petroleum exploration: oil from chalks, a modern miracle? *AAPG Bull.*, 61, 982–1009.

Sheldon, H., Wheeler, J., Worden, R.H. and Cheadle, M.J. (2003) An analysis of the roles of stress, temperature, and pH in chemical compaction of sandstones. *J. Sed. Res.*, 73, 64–71.

Sheppard, T.H. (2002) Stylolite development at sites of primary and diagenetic fabric contrast within the Sutton Stone (Lower Lias), Ogmore-by-Sea, Glamorgan, UK. *Proc. Geol. Assoc.*, 113, 87–109.

Simpson, J. (1985) Stylolite-controlled layering in an homogeneous limestone: pseudo-bedding produced by burial diagenesis. *Sedimentology*, **32,** 495–505.

Tanaka, M. and **Takahashi, K.** (2000) The identification and characterization of silicate complexes in calcium chloride solution using fast atom bombardment mass spectrometry. *Anal. Chim. Acta*, **411,** 109–119.

Tanaka, M. and **Takahashi, K.** (2002) Characterization of silicate monomer with sodium, calcium and strontium but not with lithium and magnesium ions by fast atom bombardment mass spectrometry. *J. Mass Spectrom.*, **37,** 623–630.

Von Breymann, M.T., Emeis, K.-Ch. and **Camerlenghi, A.** (1989) Geochemistry of sediments from the Peru upwelling area: results from ODP Sites 680, 682, 685, and 688. *Proc. ODP Sci. Results*, **112,** 491–503.

Weyl, P.K. (1959) Pressure solution and the force of crystallization – a phenomenological theory. *J. Geophys. Res.*, **64,** 2001–2025.

Winterer, E.L. et al. (1971) *Init. Rep. DSDP, 7.* US Govt. Printing Office, Washington, DC. 930 pp.